2014

Functional significance of the interaction between inducible costimulator (ICOS) and its ligand (ICOSL)

BOSTON UNIVERSITY

SCHOOL OF MEDICINE

Thesis

FUNCTIONAL SIGNIFICANCE OF THE INTERACTION BETWEEN INDUCIBLE COSTIMULATOR (ICOS) AND ITS LIGAND (ICOSL)

by

ELIZABETH KIERAS

B.S., Providence College, 2003

Submitted in partial fulfillment of the

requirements for the degree of

Master of Arts

2014

Approved by

First Reader _____

Gerald Denis, Ph.D.
Associate Professor of Medicine and Pharmacology

Second Reader _____

Lori Fitz, Ph.D.
Adjunct Professor of Pharmacology
Associate Research Fellow, Pfizer

ACKNOWLEDGMENTS

I would like to thank all of my Pfizer colleagues and Boston University (BU) professors and advisors who have helped me to greatly expand my scientific knowledge and capacity to understand the vast array of techniques available in research and how to ask the right questions in order to perform meaningful scientific research. Prior to embarking on this program, I felt very rusty in the biology that I had learned in my undergraduate studies and uncertain about the appropriate research questions to ask to advance biology and drug discovery. My tenure at Wyeth/Pfizer and in the BU Pharmacology and Experimental Therapeutics department have greatly increased my scientific awareness and understanding, and have given me much more confidence to contribute to my ideas in discussions with other scientists.

In particular, I would like to thank Lori Fitz, my manager at Pfizer for the past 4 years and my mentor in the BU Pharmacology program. Over this time, Lori has been a voice of practicality and encouragement, guiding me into areas where I need to advance, and congratulating me on my successes. I am hugely grateful for the support that she has provided to me. I would also like to thank my former managers at Wyeth/Pfizer, including Désirée Tsao, Neil Wolfman, and Will Somers who supported my desire to enroll in the BU Pharmacology program and allowed me the flexibility in my job to continue in both capacities.

I would like to thank the many BU professors and classmates who have helped me through my courses and on my committees to greatly expand in my

knowledge of pharmacology, inflammation, drug discovery and other relevant scientific fields. In particular, I would like to thank Dr. Terrell Gibbs who served on my qualifying exam committee (QEC) and as chair of my dissertation advisory committee (DAC) for providing guidance on my proposed experimental design and for his instruction on the theoretical principles of ligand binding in the Molecular Neuropharmacology class. I would like to thank Dr. Gerald Denis for serving on my DAC and as first reader of my master's thesis, and for his guidance in translationally relevant experiments in immunology. I would like to thank Dr. Carol Walsh for her advisorship throughout the program, for her instruction in the principles of pharmacokinetics and treatments for inflammatory diseases, and for her service on my QEC. I would like to thank Dr. Benjamin Wolozin for his instruction in the Advanced General Pharmacology class and leadership of my QEC and Dr. Alan Herbert for his service on my DAC. Finally, I would like to thank Dr. David Farb for his support of Pfizer students in the Pharmacology & Experimental Therapeutics department and for his overall leadership of the department.

I would also like to thank Pfizer colleagues who have contributed to my research on the ICOS: ICOSL interaction. I would like to thank Matthew Whitters and the late Yuang-Taung Juang for engaging in in-depth conversations about meaningful biology of the ICOS: ICOSL interaction that remained to be studied, their critique of my research proposal, and their leadership of Pfizer's internal program targeting ICOSL. I would like to thank Paul Wu for sharing his expertise

and mentorship in all molecular biology techniques that have been useful for this research and for expressing the sICOSL construct that I used in my experiments. I would like to thank Yanyu Zhang for teaching me how to use the SEC-MALS instrumentation used to characterize the aggregation state of sICOSL for this project. I would like to thank members of my own group including Jonathan Brooks, Julia Downall, and Julie Lee for training me to use the Biacore SPR binding platform and for their support through the years. I would like to thank Deborah Luxenberg for teaching me the cell culture skills that I needed to perform this research. I would like to thank colleagues at Sapidyne, Inc., in particular Lindsey Hunt and Elizabeth Hopkins, for providing training on the KinExA platform. I would also like to thank colleagues who have contributed reagents that have been useful to this project, including Darren Ferguson and Jill Wright for purification of the sICOSL protein.

I would be remiss not to mention the support and camaraderie I have received from my fellow colleagues and classmates at both Pfizer and BU who I have gone through this program alongside, and who have provided a huge amount of moral support and encouragement when the demands of both programs felt high; in particular Paul Wu, Joy Miyashiro, and Nicole Piché-Nicholas.

Finally, I would like to thank my husband, Matthew Kieras for his support of my participation in this program and for his understanding when my personal life had to be set aside in order to meet the demands of this program. I would

also like to thank my son, Jack, for bringing so much joy and meaning to life in the nearly two years since he arrived. The support of both of our immediate families has also been an invaluable resource in shaping the person I've become and in helping me to balance my responsibilities at home with those at work and at school. I am extremely grateful to be a part of all of these different communities that have enriched my life.

FUNCTIONAL SIGNIFICANCE OF THE INTERACTION BETWEEN INDUCIBLE COSTIMULATOR (ICOS) AND ITS LIGAND (ICOSL)

ELIZABETH KIERAS

ABSTRACT

Background

Inducible costimulator (ICOS) and its ligand (ICOSL) are a pair of costimulatory molecules that co-localize in germinal centers (GC). This interaction is critical for the maturation of GC B cells to affinity-matured memory B cells and long-lived plasma cells. Both ICOS and ICOSL are implicated in systemic lupus erythematosus (SLE). It is known that ICOSL sheds from the cell membrane and that the soluble form of ICOSL (sICOSL) is elevated in SLE; though the function of sICOSL is poorly understood. While it is known that binding of ICOSL on antigen-presenting cells (APC) to ICOS on T cells leads to cell signaling resulting in T cell activation and differentiation, there is also some preliminary evidence that reverse signaling may also occur through ICOSL in APCs. The binding interaction between ICOS and sICOSL has not been fully characterized and is important to understand if either molecule is to be targeted therapeutically. *The hypothesis evaluated in this study was that the ICOS: ICOSL interaction is a potent and critical mediator of proinflammatory signaling and immune activation that functions both via activated T cell-mediated forward signaling and APC-mediated reverse signaling mechanisms and that ectodomain shedding of ICOSL is a protective mechanism that leads to down-regulation of the proinflammatory*

signaling cascade initiated by this interaction. The aim of this thesis is to characterize the binding interaction between ICOS and ICOSL and to provide a review of the literature and discuss future work that would enhance the biological understanding of this interaction and its role in lupus and other autoimmune diseases.

Methods

The binding interaction between ICOS and ICOSL was characterized using both soluble proteins and cells with expressed recombinant proteins. Purified soluble ICOSL (sICOSL) was characterized using size-exclusion chromatography multiangle light scattering (SEC-MALS). Surface plasmon resonance (SPR) was used to measure the binding affinity between sICOSL and human ICOS fused to the fragment crystallizable (Fc) portion of an immunoglobulin molecule (hICOS.Fc). The binding interaction was further characterized to account for avidity between hICOS.Fc and sICOSL and between hICOS.Fc and ICOSL expressed recombinant on the cell surface using a solution-based binding method.

Results

Expressed recombinant and purified sICOSL dimerized over time and with increasing temperatures. The sICOSL: hICOS.Fc interaction did not follow a typical 1:1 binding interaction. In-solution binding experiments resulted in a tighter equilibrium dissociation binding constant (K_D) than the surface-based results obtained by SPR. The K_D for hICOS.Fc binding to human ICOSL

(hICOSL) expressed on cells agreed well with the K_D for hICOS.Fc to the soluble protein, indicating that the in-solution binding measurement may measure binding avidity rather than affinity and that this may be the more physiologically relevant interaction.

Conclusions

I show in the experimental part of this study that the interaction between ICOS and ICOSL is quite potent and that much of the binding strength is due to avidity, or the combined strength of multiple parts of the molecules interacting with one another, rather than the affinity alone. As this interaction is implicated in SLE pathogenesis, it would be useful to develop a clearer understanding of the most relevant physiological form of these molecules (soluble or transmembrane) and of the biological signaling events that are initiated via this interaction in order to determine whether targeting ICOS or ICOSL may be therapeutically viable approaches.

TABLE OF CONTENTS

LIST OF TABLES

LIST OF FIGURES

LIST OF ABBREVIATIONS

ANA ..... antinuclear antibody

APC ..... antigen-presenting cell

BCR ..... B cell receptor

BILAG ..... British Isles Lupus Assessment Group

BLyS ..... B Lymphocyte Stimulator

BSA ..... bovine serum albumin

BU ..... Boston University

CCR7 ..... C-C chemokine receptor type 7

CD ..... Cluster of Differentiation

CD40L ..... CD40 ligand

CHO ..... Chinese hamster ovary

CM5 ..... carboxymethylated dextran 5

CMF ..... calcium and magnesium free

CTLA-4 ..... cytotoxic T lymphocyte-associated antigen 4

CXCR5 ..... C-X-C chemokine receptor type 5

DAC ..... dissertation advisory committee

DC ..... dendritic cell

DMARD ..... disease-modifying antirheumatic drug

DME ..... Dulbecco's Modified Eagle's Medium

DMSO ..... dimethyl sulfoxide

DR2 ..... DRB1*1501/DRA0101

dsDNA ..... double-stranded deoxyribonucleic acid

EDC .....*N*-ethyl-*N*'-(30-dimethylaminopropyl) carbodiimide

EDTA ..... ethylenediaminetetraacetic acid

ENA .....extractible nuclear antigen

Fc .....fragment crystallizable

FcγRIIB ..... Fc gamma receptor IIB

fM ..... femtomolar

Foxp3 ..... forkhead box P3

GC .....germinal center

HEK293T cells.....Human Embryonic Kidney 293 T cells

HEPES ..... 4-(2-hydroxyethyl)-1-piperazineethanesulfonic acid

hICOS.....human ICOS

hICOSL..... human ICOS ligand

hr ..... hour

ICOS..... inducible costimulator

ICOSL..... inducible costimulator ligand

IDO .....indoleamine 2,3-dioxygenase

IFN..... interferon

Ig ..... immunoglobulin

IgC.....constant immunoglobulin

IgE ..... immunoglobulin E

IgV .....variable immunoglobulin

IL ..... interleukin

IVIG ..... intravenous immunoglobulins

k_a ..... association rate constant

k_d ..... dissociation rate constant

K_D ..... dissociation binding constant

KCl ..... potassium chloride

kDa ..... kilodalton

KH_2PO_4 ..... monopotassium phosphate

KinExA ..... kinetic exclusion assay

M ..... molar

mAb ..... monoclonal antibody

MALS ..... multi-angle light scattering

MAPK ..... mitogen-activated protein kinase

MHC ..... major histocompatibility complex

min ..... minute

mg ..... milligram

$MgCl_2$ ..... magnesium chloride

mL ..... milliliter

mM ..... millimolar

mRNA ..... messenger ribonucleic acid

NaCl ..... sodium chloride

Na_2HPO_4 ..... disodium phosphate

NaOH ..... sodium hydroxide

NF-κB .....nuclear factor kappa-light-chain-enhancer of activated B cells

NHS ..... *N*-hydroxysuccinimide

nM ..... nanomolar

NSAID ..... non-steroidal anti-inflammatory drug

NSB .....non-specific binding

PBS ..... phosphate buffered saline

PD-1 .....programmed cell death protein 1

PGA..... Physician Global Assessment

pM .....picomolar

PI3K..... phosphoinositide 3-kinase

PMA..... phorbol-12-myristate-13-acetate

PMMA.....polymethylmethacrylate

QEC..... qualifying exam committee

R..... receptor

RA .....rheumatoid arthritis

RU ..... response units

s.....second(s)

SDS-PAGE ..... sodium dodecyl sulfate polyacrylamide gel electrophoresis

SEC ..... size-exclusion chromatography

sICOSL..... soluble ICOSL

SLE..... systemic lupus erythematosus

SLEDAI.....SLE Disease Activity Index

SNP ..... single nucleotide polymorphism

SPR ..... surface plasmon resonance

sTNF.....soluble TNF

T_{H1} .....T helper 1 cell

T_{H2} .....T helper 2 cell

T_{H17}.....T helper 17 cell

T_{FH} .....follicular helper T cell

T_{REG} .....regulatory T cell

TACE..... TNF-α converting enzyme

TCR .....T cell receptor

TGFβ .....transforming growth factor beta

TIMP-3..... tissue inhibitor of metalloproteinase 3

TNF .....tumor necrosis factor

Tris ..... tris(hydroxymethyl)aminomethane

Trp ..... tryptophan

µg ..... microgram

µL .....microliter

µM .....micromolar

v.....volume

w.....weight

INTRODUCTION

Costimulation via CD28- and B7-family members

The interaction between inducible costimulator (ICOS) and its ligand (ICOSL) is part of a costimulatory event that is required for T cell activation and differentiation to occur. ICOS is a member of the CD28 family of costimulatory receptors expressed on T cells. ICOSL is a member of the B7 family of ligands expressed on antigen presenting cells (APC).

Costimulatory signaling is one of three signals that are required for T cell activation. Signal 1 is the presentation of antigen peptide via major histocompatibility complex (MHC) on the surface of an APC to the T cell receptor (TCR) on a naive $CD4^+$ or $CD8^+$ T cell. Signal 2 is the interaction between surface-bound costimulatory molecules on APCs with their receptors on T cells. Signal 3 is mediated by soluble cytokines which control differentiation into different effector T cells. In the absence of the second costimulatory signal, the T cell enters an anergic state or undergoes apoptosis (Murphy *et al*. 2008: 324-325). Anergy is a tolerance mechanism in which the lymphocyte is hyporesponsive and functionally inactivated following an antigen encounter, but remains alive for an extended period of time (Schwartz, 2003). Apoptosis, also known as programmed cell death, includes characteristic cellular changes including blebbing, shrinking, and fragmentation of the nucleus and chromosomal DNA (Elmore, 2007).

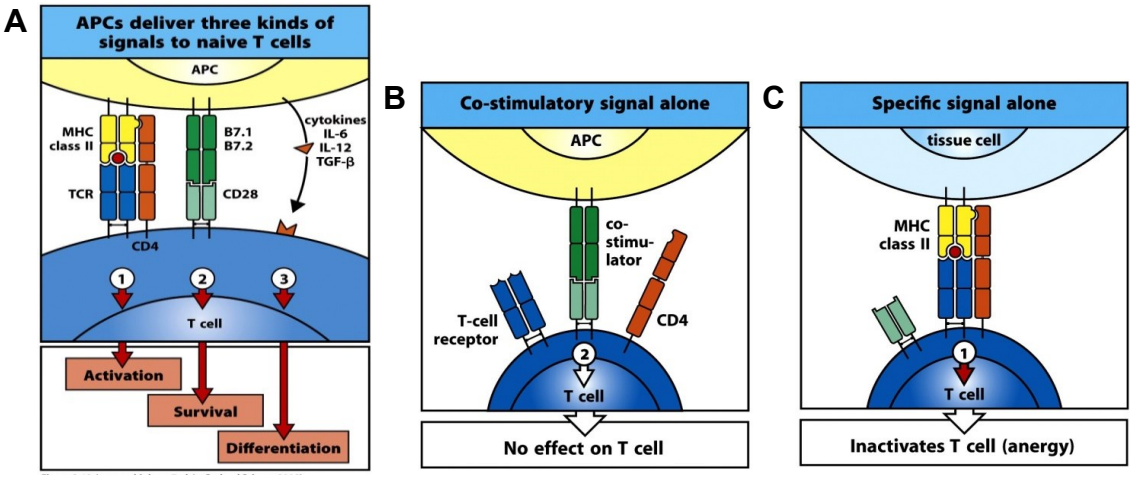

Figure 1: Signals Required for T Cell Activation. **A**. Antigen-presenting cells deliver three kinds of signals to naïve T cells. Signal 1 is the presentation of antigen peptide via the MHC to the TCR. Signal 2 is the binding of costimulatory ligands on APCs to costimulatory receptors on T cells. Signal 3 is mediated by soluble cytokines which lead to differentiation of activated T cells into effector T cells. **B**. In the absence of Signal 1, Signal 2 does not lead to T cell activation or differentiation. **C**. Signal 1 in the absence of Signal 2 leads to T cell inactivation, or anergy. (Murphy *et al.* 2008, Figures 8.19 and 8.23).

The classic costimulatory event is B7-1 or B7-2 binding to Cluster of Differentiation 28 (CD28) on T cells. This leads to naive T cell activation and increased interleukin-2 (IL-2) production primarily due to messenger ribonucleic acid (mRNA) transcription and stabilization. IL-2 further activates T cells through binding to the IL-2 receptor (IL-2R), leading to increased T cell proliferation (Murphy *et al*. 2008: 345-346). In addition to the activating costimulatory receptor, CD28, activated T cells also constitutively express cytotoxic T lymphocyte-associated antigen 4 (CTLA-4), a CD28 family member, which also binds to B7-1 and B7-2, but with a higher affinity than CD28 (van der Merwe, 1997). Engagement of B7-1 or B7-2 with CTLA-4 initiates inhibitory signals to T

cells, limiting further activation via CD28 (Chambers, 2001). Thus, CTLA-4 has an important role in down-regulating inflammation. CD28 is constitutively expressed on resting T cells and B7-2 is induced rapidly following antigen presentation to APCs, whereas expression of B7-1 and CTLA-4 is delayed for approximately 24 to 48 hours into the immune response (Collins *et al*., 2002). Thus the B7-2: CD28 interaction is likely the primary costimulatory interaction used to activate T cells following antigen presentation and the higher affinity B7-1: CTLA-4 interaction is likely a negative feedback mechanism to inhibit immune over-proliferation that would occur due to unchecked CD28 signaling. As evidence of its negative feedback role, CTLA-4 deficient mice die within several weeks of birth due to massive lymphoproliferation, infiltration, and multi-organ destruction (Waterhouse *et al*., 1995). In keeping with the beneficial inhibitory effects of CTLA-4, the drug abatacept (CTLA-4-Ig, ORENCIA®) has been approved for the autoimmune disease rheumatoid arthritis (RA) and for transplant rejection where inhibiting an overactive immune response is critical to managing disease (Gizinski *et al*., 2010).

ICOS: ICOSL Interaction

ICOS was first identified in 1999 as the third member of the CD28 costimulatory family (Hutloff *et al*., 1999). ICOS shares 24% sequence identity with CD28 and 17% identity with CTLA-4. ICOS is a disulfide-linked homodimer, expressed on the surface of T_{H1}, T_{H2}, T_{H17}, T_{FH}, and T_{REG} activated $CD4^+$ and

$CD8^+$ T cells (Hutloff *et al*., 1999; Simpson *et al*., 2010). Unlike CD28 and CTLA-4, a single ligand has been identified for ICOS: the B7 family member ICOSL, also known as ligand of ICOS (LICOS), B7h, B7RP-1, B7-H2, and GL50 (Ling *et al*., 2000). ICOSL is expressed on B cells, dendritic cells (DC), macrophages, and multiple non-lymphoid tissues, including tumor necrosis factor alpha (TNF-α)-activated fibroblasts, intraepithelial lymphocytes, brain tissue, lymph node and thymic tissue, lung, heart, kidney, liver, peritoneum, and testes (Aicher *et al*., 2000; Ling *et al*., 2000; Chambers, 2001).

ICOSL binds to ICOS via multiple residues within its variable immunoglobulin (IgV) domain. In particular, the FDPPPF[1] amino acid motif in the IgV domain is critical for forming contacts with ICOSL. This motif is homologous to the MYPPPY[1] motif on CD28 and CTLA-4, which binds B7-1 and B7-2. The constant immunoglobulin (IgC) domain in ICOS has been shown to be critical for maintaining the structural integrity of the molecule and preventing nonspecific aggregates from forming (Chattopadhyay *et al*., 2006). Signaling through ICOS in T cells has been fairly well characterized. Like CD28, ICOS stimulation following ICOSL ligation sends an activating signal to T cells. This leads to further T cell activation and differentiation and regulates cytokine and Ig production. ICOS signaling plays a critical role in B cell differentiation, Ig class switching, germinal center formation, memory B cell development, and production of autoimmune antibodies by self-reactive B cells (Greenwald *et al*.,

[1] 1-Letter amino acid abbreviations can be found in Appendix.

2005; McAdam *et al*., 2001). Also like CD28, the intracellular domain of ICOS associates with the p85 subunit of phosphoinositide 3-kinase (PI3K) via the YMFM[1] motif in the intracellular tail. This is similar to the YMNM[1] motif in CD28. The change in this motif, however, abolishes binding to growth factor receptor-bound protein 2 (Grb-2), in which case the asparagine (N) residue in the YMNM[1] motif of CD28 appears to be critical for Grb-2 binding (Coyle *et al*., 2000).

A major difference between ICOS and CD28 signaling is that ICOS does not induce IL-2 production but does induce high levels of IL-10 production, leading to T_{REG} regulation, T cell tolerance, and autoimmunity (Greenwald *et al*., 2005). Additionally, ICOS is important for the induction of interferon gamma (IFN-γ), TNF-α, IL-4, IL-5, IL-13, and IL-21 (Simpson *et al*., 2010). ICOS costimulation appears to be critical at late stages in the immune response, suggesting that its inhibition may provide therapeutic benefit in treating diseases in which activated T cells are believed to contribute to disease progression (Coyle *et al*., 2000).

Within secondary lymphoid organs, lymphocytes segregate into discrete B and T cell zones, or follicles. Antigen activation increases the expression of C-C chemokine receptor type 7 (CCR7) on B cells, which causes migration to the follicular interface. ICOS on T_{FH} cells interacts with ICOSL on B cells within germinal centers to produce memory B cells and plasma cells, important components of adaptive immunity. T_{FH} cells are characterized by high

[1] 1-Letter amino acid abbreviations can be found in Appendix.

expression of C-X-C chemokine receptor type 5 (CXCR5), programmed cell death protein 1 (PD-1), and IL-21. ICOSL and CD40 ligand (CD40L) have both been identified as required for T_{FH} cells and for germinal center formation.

ICOSL knockout mice are viable and do not display any obvious physical or behavioral abnormalities. Homozygous knockouts show impaired T and B cell dependent immunological responses. In particular, these mice produce fewer and smaller germinal centers upon antigen challenge and display lower immunoglobulin E (IgE) levels than wild-type mice in a murine asthma model. T cells from these mice produce less IL-4 and IL-10 than wild-type animals and B-cell isotype switching is also impaired (B6.129P2-*Icosl*$^{tm1Mak/J}$, 2014).

Role of ICOS and ICOSL in SLE

Systemic lupus erythematosus (SLE) is a chronic inflammatory disease affecting the skin, joints, kidneys, lungs, and nervous system. It is a heterogeneous autoimmune disorder, in which different patients exhibit different symptoms and disease severity (Systemic Lupus Erythematosus (Lupus), 2014). It is estimated that 1.5 million Americans and 5 million people worldwide suffer from lupus, with over 16,000 new cases reported annually in the United States (What is lupus?, 2014). The average annual cost per lupus patient is $5,000 - $19,000 greater than the average annual medical cost for people without lupus and is much higher for patients who suffer from lupus nephritis (Assessing the Cost of Lupus, 2014).

Lupus is a chronic disease with periods of flares, or worsening symptoms, and remission. It can range from mild to life-threatening. Lupus treatment has improved considerably over the past several decades. In the 1950s, most people diagnosed with SLE live less than 5 years, whereas today over 90% survive for more than 10 years, and 80-90% of SLE patients live a normal lifespan. In late stages of disease, mortality risk if five-fold higher than the normal population and is attributed mainly to heart disease from atherosclerosis, as well as increased risks of infections and cancer (Systemic lupus erythematosus, 2014). Many with lupus can lead relatively normal lives if properly treated. However, quality of life is often affected due to symptoms such as fatigue and joint pain, and unpredictable flare periods. Not all patients respond to current treatments and symptoms often worsen over time leading to complications such as organ damage, atherosclerosis, and kidney disease (Systemic Lupus Erythematosus (Lupus), 2014). While SLE is not one of the leading causes of death worldwide and mortality rates due to lupus are fairly low, it is a chronic disease that affects overall quality of life, and in many cases, treatments are still inadequate at controlling the disease.

Most lupus patients have autoantibodies directed against antinuclear antigens, including double-stranded DNA (dsDNA). Lupus has been called the great imitator as it is characterized by many different symptoms, none of which are specific to lupus alone. These include fever and fatigue, arthritis, malar rash, sores in the mouth and nose, hair loss, seizures and mental disorders, blood

clots and stroke, miscarriage, blood or protein in urine, and low blood counts (Systemic Lupus Erythematosus (Lupus), 2014).

Despite advances in therapy for SLE, the management and control of disease activity remains challenging. SLE treatment depends on a patient's symptoms and disease severity. There are several different available assessments to measure disease severity in lupus. Among these, some of the most widespread are the Physician Global Assessment (PGA), the British Isles Lupus Assessment Group (BILAG), and the SLE Disease Activity Index (SLEDAI). The PGA is a global assessment based on a visual analog scale from 0-3 of relative change over the last 2 weeks, where mild flare scores 1 point, moderate flares score 2.0-2.5 points, and severe flares score a 3. The BILAG index evaluates disease activity over the past month in 8 separate organ systems, comprising a total of 86 items to be scored with a maximum score of 81. The SLEDAI measures disease activity over the past 10 days and includes 24 weighted clinical and laboratory items with a score ranging from 0-105 (Luijten *et al*., 2012).

Serologic diagnosis is based on positive results from antinuclear antibody (ANA) and anti-extractable nuclear antigen (ENA) tests as well as at least 4 out of 11 clinical symptoms (Systemic Lupus Erythematosus (Lupus), 2014). Treatments include analgesics such as non-steroidal anti-inflammatory drugs (NSAIDs) and opioids to relieve pain, disease-modifying antirheumatic drugs (DMARDs) such as hydroxychloroquine, corticosteroids, and cyclosporine to

suppress the immune response, and biologics such as intravenous immunoglobulins (IVIG) and the recently approved anti-B Lymphocyte Stimulatory (BLyS) inhibitor, Benlysta (Hahn, 2011).

For reasons that are not well understood, lupus and most other autoimmune diseases are much more prevalent in women than in men. In general, women are 2.7 times more likely than men to develop an autoimmune disease. Women are 9 times more likely than men to develop SLE (Quintero *et. al*., 2012). It is believed that increases in female hormones, such as estrogen, may trigger lupus flares, and that the increased number of X chromosomes in females *vs*. males may account for this discrepancy between the sexes.

Onset in women is typically observed during reproductive ages and may be associated with rises in hormones such as estrogen, progesterone, and prolactin, which have been shown to elicit a T_{H2} immune response. SLE symptoms often worsen during pregnancy. It appears that autoimmunity is related to the genes expressed on the X chromosome. For example, males with two X chromosomes (XXY males) are more likely to develop autoimmune disease than typical XY males. Females who have only a single X chromosome (X0) are less likely to develop autoimmune disease than typical females with two X chromosomes (XX). Females who do not show skewed X chromosome inactivation, meaning that one X chromosome is inactivated in many more cells than another, are also more prone to autoimmune disease. This often occurs due to a mutation on one X chromosome or due to age (Quintero *et al*., 2012).

ICOS costimulation is implicated in the pathogenesis of SLE. A family-based association study identified single nucleotide polymorphisms (SNP) within the *CD28-CTLA4-ICOS* locus that were increased in SLE families compared to controls. A 3' flanking region of CTLA-4 extending into the ICOS promoter was confirmed to be important region for SLE association (Cunninghame Graham *et al*., 2006). In addition, $ICOS^+$ T cells are increased in patients with active SLE compared to patients with inactive SLE or healthy controls (Zhiping *et al*., 2005). Elevated levels of $CD4^+ICOS^+Foxp3^+$ T cells in SLE patients correlated with increased plasma levels of IL-10 and transforming growth factor beta (TGF-β), which are known to be up-regulated by ICOS signaling (Liu *et al*., 2011; Greenwald *et al*., 2005). Increased soluble ICOSL (sICOSL) is observed in the plasma of active SLE patients *vs*. inactive SLE patients, RA patients, or healthy controls (Her *et al*., 2009). Finally, the *Sanroque* mouse, which contains a mutation in Roquin, a gene that normally limits ICOS expression by degradation of *Icos* mRNA, is found to exhibit high autoantibody titers and pathology consistent with lupus (Yu *et al*., 2007). Together, these results suggest that signaling through the ICOS: ICOSL interaction is implicated in autoimmune disease, and specifically SLE.

The signaling initiated upon ICOS: ICOSL interaction is dependent on cell: cell contact between APCs that express ICOSL and T cells that express ICOS. This is thought to occur in the context of other adhesion and costimulation events

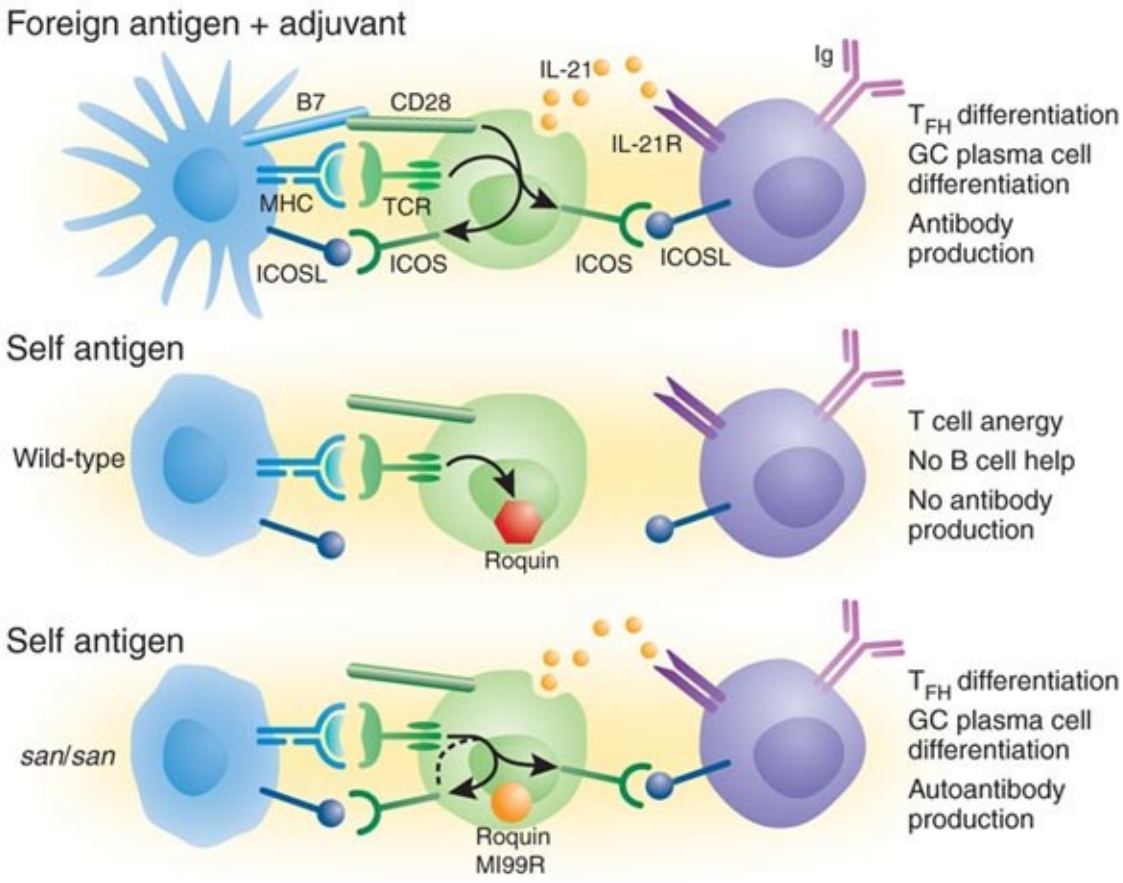

Figure 2. Role of ICOS Signaling in Autoimmune Disease. (Heissmeyer *et al*., 2005, Figure 1).

during immune activation. APCs are activated by contact with pathogens present in complexes of the foreign peptide and MHC. Activated APCs up-regulate the expression of B7 and ICOSL. These ligands in turn signal to T cells. The costimulatory signal from B7 through CD28 on T cells up-regulates ICOS expression on T cells and leads to the differentiation of T_{FH} cells. ICOS-expressing T_{FH} cells produce IL-21 and help B cells to generate antigen-specific antibodies. Roquin down-regulates ICOS expression in wild-type T cells. In

san/san T cells from *Sanroque* mice, ICOS expression is not repressed, leading to unregulated autoantibody production by B cells (Heissmeyer *et al*., 2005). Without Roquin present to inhibit ICOS expression, a feed-forward loop can emerge, in which activated T_{FH} cells provide constant stimulation to GC B cells, leading to increased B cell maturation and antibody production, which can in turn lead to the production of self-reactive autoantibodies, which are the primary pathogenic mechanism of SLE and other autoimmune diseases. It is possible that Roquin is more highly expressed in males than in females, or that it is inhibited by estrogen expression and contributes to the increased prevalence of SLE in females *vs*. males.

Reverse signaling identified for B7 family members

In addition to their roles in T cell signaling, the related costimulation molecules CD28 and CTLA-4 have also been shown to initiate reverse signaling cascades through their ligands B7-1 and B7-2 in APCs. CTLA-4 activates indoleamine 2,3-dioxygenase (IDO) and increases tryptophan (Trp) catabolism in APCs, which leads to decreased T cell proliferation. Through its interaction with B7, CTLA-4 has been shown to induce transcription of *Ifng* in a nuclear factor kappa-light-chain-enhancer of activated B cells (NFκB)- and p38 mitogen-activated protein kinase (MAPK)-dependent manner. Interferon-gamma (IFN-γ) then acts to induce expression of IDO, which is responsible for Trp catabolism (Grohmann *et al*., 2002). This reverse signaling has been shown to be part of the mechanism

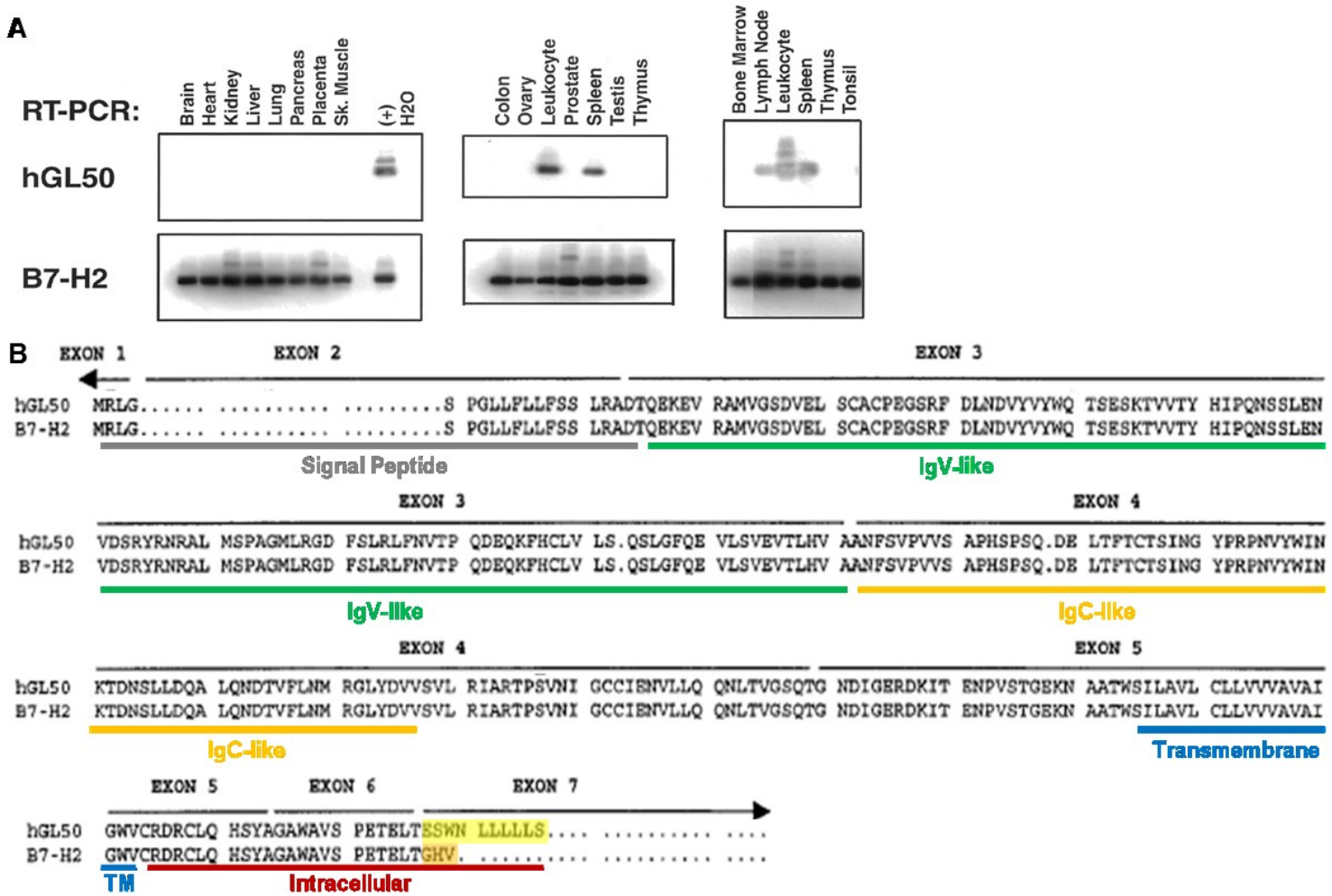

Figure 3. ICOSL splice variants. **A.** Expression of splice variants by RT-PCR. (Ling *et al.*, 2001, Figure 4). **B.** Sequence alignment of human splice forms. Domain predictions shown are based on modeling in Vector NTI software (Life Technologies). (Modified from Ling *et al.*, 2001, Figure 2).

of action of abatacept (Kremer *et al*., 2006). CD28 reverse signaling through B7-1 and B7-2 on DCs induces p38 MAPK-dependent expression of IL-6 and IFN-γ (Orabona *et al*., 2004).

There is some reason to believe that reverse signaling may also occur through the ICOS: ICOSL interaction. There are two different splice variants of ICOSL. The more prevalent splice variant, B7-H2, is ubiquitously expressed and was found in brain, heart, lung, kidney, liver, lung, pancreas, muscle, gastrointestinal tissue, sex organs, and immune tissues. The second splice variant, GL50, is only expressed in immune tissues, including leukocytes, spleen, and lymph nodes (Figure 3A). The two splice forms differ only by 10 amino acids in their C-terminal intracellular tails (Figure 3B), (Ling *et al*., 2001). Tang *et al*. show that ICOS-Ig binding to ICOSL on immature mouse DCs enhances p38 MAPK-dependent IL-6 expression and increases in surface expression of B7-1, B7-2, and CD83 on DCs following ICOS-Ig stimulation (Tang *et al*., 2009).

Ectodomain Shedding

Ectodomain shedding, the release of the extracellular domain of protein through limited proteolysis, is a regulatory mechanism for transmembrane proteins. In the B7 family, ectodomain shedding is unique to ICOSL. The mechanisms of ectodomain shedding are as diverse as the proteins that it regulates (Arribas and Borroto, 2002). The TNF family, which also plays a role in costimulation, also undergoes ectodomain shedding. These proteins are cytokines that are

synthesized as transmembrane proteins. The receptor-binding domains of these proteins are released extracellularly via ectodomain shedding. In the case of TNF-α, the protein responsible for this cleavage event is TNF-α converting enzyme (TACE), also known as ADAM17. TACE is a membrane-bound disintegrin metalloproteinase. It is inhibited by tissue inhibitor of metalloproteinase 3 (TIMP-3) and synthetic metalloproteinase inhibitors (Amour *et al*., 1998).

There is evidence for ICOSL shedding in mice and in humans, but the importance of shedding is not well understood. In mouse models of immune activation, ICOSL is rapidly shed from B cells following ICOS binding or B cell receptor (BCR) engagement (Logue *et al*., 2006). While mouse models are useful for developing an initial understanding of the human immune system, many cell types and pathways which are found in mouse are not replicated within humans. Therefore, it is always important to replicate findings from mice within human cells and systems before claiming translational significance (Mestas and Hughes, 2004). ICOSL down-regulation on human peripheral blood B cells is observed following co-culture with ICOS-transfected cells for 48 hours *in vitro*. Interestingly, other costimulatory ligands, CD40, B7-1, and B7-2, were not down-regulated following ICOS stimulation, suggesting the ICOSL shedding is specific to this molecule, and possibly important for its regulation. Peripheral blood $CD4^+$ and $CD8^+$ T cells from SLE patients had higher ICOS expression whereas $CD19^+$ B cells had lower ICOSL expression compared to healthy controls (Hutloff *et al*.,

2004). It is not known whether these decreased ICOSL levels are due to ectodomain shedding, or another mechanism. One hypothesis is that shedding may be protective, as shed ICOSL may diffuse away from the GC interface, leading to decreased signaling through ICOS: ICOSL. This is consistent with the observation of decreased expression of surface ICOSL as soluble ICOSL levels increase (Her *et al*., 2009).

Hypothesis

There is some evidence that in addition to the well-established signaling that occurs in T cells via ICOSL binding to ICOS that reverse signaling also occurs in APCs. Previous studies show that the ICOS: ICOSL interaction is important in germinal center formation and downstream antibody production. ICOSL sheds from the cell membrane and the function of this form is poorly understood. sICOSL is present in the circulation and is at higher than normal levels in the plasma of SLE patients (Her *et al*., 2009). The binding interaction between shed ICOSL and ICOS is unclear. One study shows that a monomeric form of ICOSL binds ICOS.Fc with a 4 μM binding affinity (Brodie *et al*., 2000). This study used a saturation binding technique that did not provide any information about the on or off rates of binding. It's also unclear if monomeric ICOSL is relevant to either the transmembrane or even the shed ICOSL form. Chattopadhyay *et al*. (2006) showed that recombinant ICOSL is primarily a dimer in solution and can form dimers and higher order oligomers on the membranes of

Human Embryonic Kidney 293 T cells (HEK293T cells). The binding interaction between ICOS and its ligand are important to define for potential drug targeting for either of these molecules. The hypothesis tested in this study was that the ICOS: ICOSL interaction is a potent and critical mediator of proinflammatory signaling and immune activation that functions both via activated T cell-mediated forward signaling and APC-mediated reverse signaling mechanisms and that ectodomain shedding of ICOSL is a protective mechanism that leads to down-regulation of the proinflammatory signaling cascade initiated by this interaction. Understanding the contributions of ICOSL to immune activation and down-regulation is important in order to develop inhibitors of this interaction.

As the ICOS: ICOSL interaction is implicated in SLE pathogenesis, it would be useful to develop a clearer understanding of the most relevant physiological form of these molecules (soluble or transmembrane) and of the biological signaling events that are initiated via this interaction in order to determine whether targeting ICOS or ICOSL may be therapeutically viable approaches. In the experimental part of this study the binding affinity for the sICOSL: ICOS interaction was measured using surface plasmon resonance (SPR). Purified expressed recombinant soluble ICOSL (sICOSL) was characterized using size-exclusion chromatography multiangle light scattering (SEC-MALS) in order to determine the oligomerization state(s) of the molecule, which helped to guide the interpretation of the binding data. Based on these results, the binding interaction was further characterized to explore the effect of

avidity on this interaction using both sICOSL and ICOSL expressed recombinant on the cell surface using a solution-based binding method. Additionally, relevant literature around reverse signaling and ectodomain shedding of ICOSL is reviewed and potential future directions for this research are explored, especially as they relate to development of therapeutics for SLE that target ICOS and ICOSL.

MATERIALS AND METHODS

Reagents

Purified recombinant human ICOS fused to the Fc portion of an immunoglobulin molecule (hICOS.Fc) expressed recombinant and purified from NS0-derived murine myeloma cells was purchased from R&D Systems. This molecule consists of the extracellular portion of ICOS (Glu21 – Phe141) fused to the hinge, CH2, CH3 domain of human IgG_1 to form a disulfide-linked homodimer with a monomeric molecular mass of 40.3 kilodalton (kDa) and 50-60 kDa by sodium dodecyl sulfate polyacrylamide gel electrophoresis (SDS-PAGE) under reducing conditions. The lyophilized protein was reconstituted to 100 μg/mL in sterile phosphate buffered saline (PBS).

Purified, recombinant monomeric hICOSL FH6, or sICOSL, expressed in a Chinese hamster ovary (CHO) suspension cell line (Icosagen) was obtained from the protein expression and purification laboratory at Pfizer. The final concentration was 2.67 mg/mL in calcium and magnesium free PBS (PBC-CMF), pH 7.2. The material was 91% monomer and 9% higher molecular weight species, by size exclusion chromatography (SEC). The molecular weight by non-reduced SDS-PAGE was 40-66 kDa. It was stable upon three freeze thaw cycles.

Cell Culture

hICOSL was expressed recombinant on the surface of CHO cells transfected with DRB1*1501/DRA0101 (DR2) chains (CHO DR2 cells) (Scholz *et al*., 1998). CHO DR2 hICOSL cells and control CHO DR2 cells were cultured in media containing 50% Dulbecco's Modified Eagle's Medium (DME)/50% Ham's F-12 medium without hypoxanthine, thymidine plus 10% fetal calf serum, 10 mM HEPES, 1% L-Glutamine, 0.22 mg/mL hygromycin B, 0.44 mg/mL G418 (geneticin), and 16.4 μg/mL gentamicin. Cells which were stored in liquid nitrogen at a concentration of approximately 1 x 10^6 cells/mL in media with 10% DMSO. Cells were thawed, and rinsed with media to remove the dimethyl sulfoxide (DMSO). Cells were diluted 15x into a T75 flask (BD Biosciences). Flasks were placed in an incubator at 37^{o}C, 5% carbon dioxide (CO_2) and were allowed to grow approximately 3 to 4 days until they were confluent. Every 3 to 4 days, media was aspirated from T75 flasks and cells were harvested via treatment with 25 mM EDTA in PBS for approximately 5 minutes. After about 5 minutes, cells were dissociated from the wall of the flask via manual force and approximately 20 mL media was added back to the flask to dilute the EDTA to an ineffective concentration. Cells were split approximately 1:30 to 1:40, depending on the level of confluence and the amount of time predicted to elapse before next harvest into 8 to 10 T-225 flasks (BD Biosciences) in order to grow a sufficient number of cells for a single KinExA experiment. On the day the experiment was

to be performed, cells were again harvested from all flasks using 25 mM EDTA and reconstituted at the maximum tolerable concentration, generally about 1 x 10^7 cells/mL or slightly less. Number of cells and viability were measured by diluting a small number of cells in trypan blue (Life Technologies) and counting using a hemocytometer and microscope.

Surface Plasmon Resonance

Binding interactions were measured by surface plasmon resonance (SPR) using a Biacore 2000 instrument (GE Healthcare, Uppsala, Sweden). All experiments were performed at 25^{o}C. Briefly, proteins were immobilized on a carboxymethylated dextran 5 (CM5) sensor chip surface (GE Healthcare) using a mixture of 5.75 mg/mL *N*-hydroxysuccinimide (NHS) and 37.5 mg/mL *N*-ethyl-*N*'-(30-dimethylaminopropyl) carbodiimide (EDC) to activate the surface followed by an anti-human IgG antibody (GE Healthcare) diluted in 10 mM sodium acetate, pH 5 on three different flow cells. The surface was subsequently blocked with 1 M ethanolamine hydrochloride-NaOH, pH 8.5. The fourth flow cell was left blank but was activated and blocked as described above. These reagents were supplied by the instrument manufacturer (GE Healthcare). The instrument running buffer and sample buffer for the immobilization and subsequent binding analyses was PBS-NET (8.1 mM Na_2HPO_4, 1.47 mM KH_2PO_4, pH 7.2, 287 mM NaCl, 2.7 mM KCl, 3.2 mM ethylenediaminetetraacetic acid (EDTA), 0.005% Tween 20). After immobilization, hICOS.Fc (R&D Systems) was captured on the

antihuman IgG sensor chip surface at a concentration of 10 μg/mL for 1 minute at a flow rate of 10 μL/min. Average surface densities on the three surfaces ranged from 87 – 239 response units (RU). After capture, various concentrations of sICOSL were each injected in triplicate at concentrations ranging from 31.25 – 1,000 nM for 2 minutes at a flow rate of 30 μL/min and were each allowed to dissociate for 5 min. All surfaces were regenerated using one 30 s pulse of 3 M $MgCl_2$ followed by a 30 s pulse of a detergent combination consisting of the following; (0.3% (w/w) CHAPS, 0.3% (w/w) zwittergent 3-12, 0.3% (v/v) Tween 80, 0.3% (v/v) Tween 20, 0.3% (v/v) Triton-X-100) at a flow rate of 50 μL/min. Data was double-referenced in Scrubber v. 2.0b software (BioLogic Software) (Myszka, 1999). The transformed data were fit to 1:1 Langmuir binding models using BiaEvaluation v. 4.1.1 (GE Healthcare) and to a 4 parameter logistic nonlinear regression model in Scrubber v. 2.0b (Biologic Software). The 1:1 kinetic binding model is based on the following equations, where A and B are individual analytes (sICOSL and hICOS.Fc) and AB is the bound product; k_a is the association rate constant, or on-rate; k_d is the dissociation rate constant, or off-rate; K_D is the dissociation binding constant, or binding affinity:

$$A + B \underset{k_d}{\overset{k_a}{\rightleftharpoons}} AB \qquad \text{and} \qquad K_D = \frac{k_d}{k_a}$$

(Önell and Andersson, 2005). The 4 parameter logistic nonlinear regression model is as follows, where A is the minimum asymptote; B is the Hill slope, which refers to the steepness of the

curve; C is the inflection point of the curve; and D is the maximum asymptote: **K_D = ((A-D)/(1+((x/C) ^B))) + D** (Motulsky 2007).

Protein Characterization

sICOSL sample was further characterized for stability by size-exclusion chromatography-multiangle light scattering (SEC-MALS) under various experimental conditions by analyzing four different samples which were treated under the following conditions: freshly thawed, stored at 4^{o}C for 24 hours, stored at room temperature for 24 hours, or stored at 37^{o}C for 24 hours. Samples were run at stock concentration, 2.67 mg/mL, in PBS-CMF. Samples were analyzed by SEC using the 2695 separation module (Waters) followed by multi-angle light scattering (MALS) using the miniDAWN TriSTAR (Wyatt Technology). SEC data was collected using Millennium software (Waters) and MALS data was collected using Astra V software (Wyatt Technology. Data was analyzed using miniDAWN and Optilab rEX (Wyatt Technology). Peaks were integrated in order to determine the relative percent of total mass recovered under each peak

In solution binding experiments (KinExA)

A KinExA instrument from Sapidyne (Boise, ID) was used for binding experiments done in solution or on cells. In this case, hICOS.Fc is the receptor and sICOSL is the ligand.

Bead preparation:

Three types of beads were coated with sICOSL to determine which offered the optimal signal for hICOS.Fc detection: polymethylmethacrylate (PMMA), azlactone, and sepharose. For immobilization, 50 μg of sICOSL prepared in 1 mL PBS, pH 7.4 was added to 200 mg PMMA beads (Sapidyne), and 20 μg of sICOSL prepared in 1 mL 50 mM sodium carbonate, pH 9.6 (coating buffer) was added to 50 mg dry azlactone beads (UltraLink®, Pierce Biotechnology) or to 1 mL of NHS-activated sepharose™ beads (pre-rinsed 5x with cold water and once with coating buffer to remove isopropanol storage solution) and the mixtures were tumbled for 2 hours at room temperature. Beads were centrifuged for approximately 30 s and then the supernatant containing coating solution was discarded and replaced with 1 mL of blocking buffer (10 mg/mL bovine serum albumin (BSA) in PBS for PMMA beads or 10 mg/mL BSA in 1 M Tris, pH 8.6 for azlactone and sepharose beads). Beads were tumbled in blocking buffer for approximately 1 hour at room temperature. The immobilized and blocked beads were added to 27 mL of sample buffer (PBS + 1 mg/mL BSA).

Signal Calibration:

In order to measure the net fluorescent signal generated by the receptor, hICOS.Fc binding to sICOSL on each bead set, a solution of 100 pM hICOS.Fc in PBS + 1 mg/mL BSA (running buffer) was prepared. Prior to beginning the automated run, each bead set was calibrated to determine a sufficient volume of

beads to fill the detection flow cell at a flow rate of 1 mL/min. For each sample, a fresh set of beads was injected, followed by the hICOS.Fc sample, followed by 1 μg/mL secondary antibody, followed by backflush of the beads and wash steps with running buffer. Net signal was calculated using the following equation: ([(Signal 100%) – (NSB)], where Signal 100% is the signal for the hICOS.Fc alone when no sICOSL is bound; and NSB refers to non-specific binding, or background binding fluorescence from the secondary labeled probe interacting with the beads or flow cell. Subsequent signal tests were performed using sepharose beads following the method described above, but coating beads with increasing concentrations up to 50 μg/mL sICOSL and at varying concentrations and volumes of hICOS.Fc.

K_D Measurement:

An experiment was performed to determine the approximate K_D for the ICOS-ICOSL interaction and to determine the preferred hICOS.Fc concentration for a full K_D experiment. A 150 pM stock solution of hICOS.Fc was prepared. sICOSL was diluted serially from 500 nM 10-fold to 50 fM into 150 pM hICOS.Fc. Solutions were incubated for 7 hours at room temperature in order to reach equilibrium. 5 mL of running buffer or sample were injected at 250 μL/min in each cycle followed by 1 μg/mL secondary antibody. All samples were run in duplicate. KinExA Pro software was used to calculate the K_D using a 4 parameter non-parametric fit model (Figure 4) and best-fit analysis using lowest sum of squares.

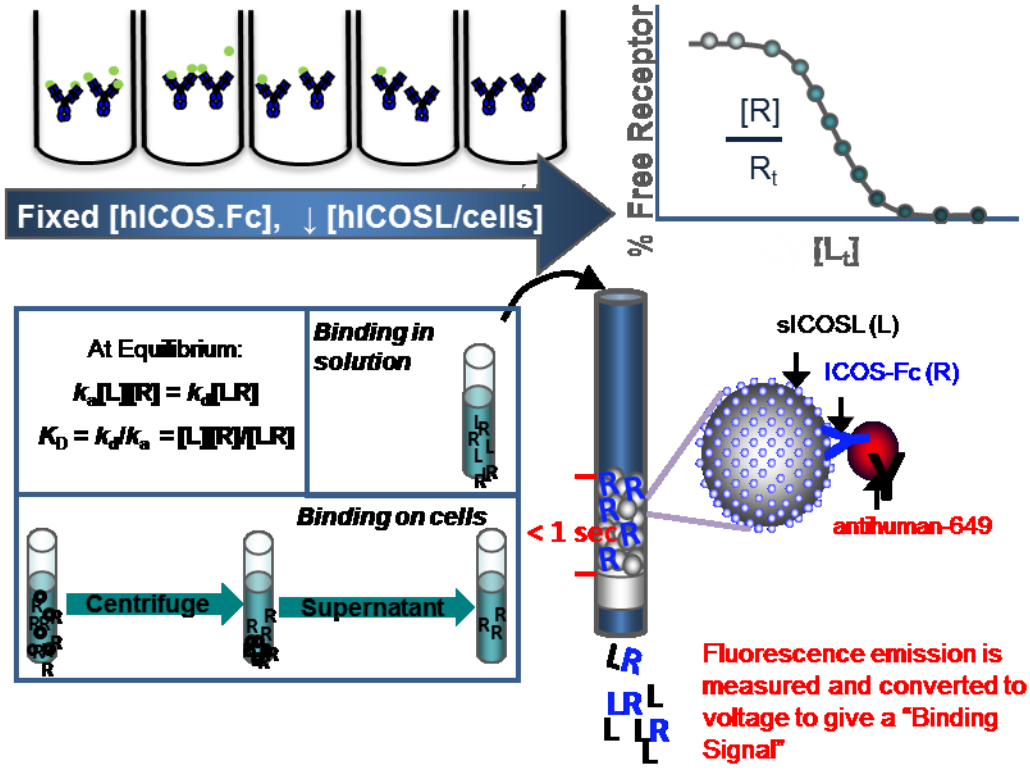

Figure 4. Equilibrium binding determination schematic via KinExA. (Modified from Sapidyne Instruments, Inc.)

Based on the results of the above experiment, subsequent experiments were performed to more precisely determine the K_D for the sICOSL: hICOS.Fc interaction. For these experiments sepharose beads were coated with 50 μg/mL sICOSL, as described above. hICOS.Fc was kept constant at 50 pM, 150 pM, or 500 pM in three independent experiments. sICOSL was titrated using 2-fold dilutions at various concentrations ranging from 2.44 pM to 40 nM. Solutions were incubated from 8 to 30 hours in order to allow each sample to come to equilibrium.

Within a single experiment, all samples were run in duplicate. Data from individual experiments was fit using KinExA Pro software, v. 3.2.6 (Sapidyne). Data from multiple experiments was fit using n-Curve Analysis software, v. 3.2.6 (Sapidyne) using the analysis method "Affinity, Standard".

Cell-based in-solution binding experiment:

A similar experiment was performed on KinExA using expressed recombinant hICOS.Fc and hICOSL expressed on CHO DR2 cells. The overall method for measuring the interaction between hICOS.Fc and hICOSL on CHO DR2 cells was run in a similar manner as described above, replacing recombinant sICOSL with CHO DR2 cells that over-express hICOSL or control CHO DR2 cells that do not express ICOSL. Starting cell concentrations ranged from 1.217×10^7 cells/mL diluted by 2- to 4-fold down to 5 cells/mL in hICOS.Fc was kept at a concentration of 100 pM or 2 nM. Cells and hICOS.Fc were rocked for approximately 18 hours at room temperature. Cell/hICOS.Fc mixture was placed in a centrifuge at 1,500 rpm (approximately 400xg) for 6 minutes to pellet the cells and any hICOS.Fc that was bound to the cells. Supernatant containing media/buffer and free hICOS.Fc was aspirated away from pellet, filtered, and put into conical tubes to be run on KinExA.

Sepharose beads were coated with 50 μg/mL hICOSL, as described above and 0.5 μg/mL secondary antibody was used to detect hICOS.Fc bound to the beads. For each sample, a fresh set of beads was injected, followed by the cell/hICOS.Fc sample (in which only free hICOS.Fc remained after

centrifugation), followed by secondary antibody, followed by backflush of the beads and wash steps with running buffer. Within each experiment, all samples were run in duplicate. Data was fit using n-Curve Analysis software, v. 3.2.6 (Sapidyne) using the analysis method "Affinity, Unknown Ligand". This analysis uses Avogadro's number to convert the concentration of hICOSL from cells/mL to a molar unit in order to determine the K_D of binding using the equation:

Molecules/cell = (Molar equivalent of cell receptor * $6.02*10^{23}$)/(cells/mL*1,000)

RESULTS

Binding Affinity between sICOSL and hICOS.Fc

Interactions between ligand and receptor costimulatory pairs are an important signal in the immune response. In the case of CD28 and its ligands, B7-1 and B7-2, the binding affinity is approximately 4 and 20 μM, respectively. In contrast these same ligands bind the coinhibitory molecule, CTLA-4, with about 10- to 20-fold stronger affinity. As CD28 is constitutively expressed on resting T cells and B7-2 is rapidly expressed on APCs, it is believed that B7-1 and CTLA-4 expression occurs after a delay of 24 to 48 hours. Crystallographic studies indicate that B7-1 tends to dimerize, whereas B7-2 does not. Additionally, CD28 homodimers are monovalent, whereas CTLA-4 is bivalent, leading to an avidity-enhanced interaction of B7-1 with CTLA-4, which has the ability to override the costimulatory interaction between B7-2 and CD28 (Collins *et al*., 2002), Thus the B7-1: CTLA-4 interaction likely overrides the costimulation driven by B7-2: CD28, attenuating an overactive immune response that left unchecked can lead to autoimmune diseases, such as SLE. In order to more fully understand the effect of immune activation contributed by ICOS: ICOSL, I designed and performed experiments to understand how their binding properties compare to these other costimulatory molecules.

My first aim was to characterize the binding interaction between ICOS and ICOSL. There is no best technique to measure binding kinetics between two

membrane-associated proteins and this is an important feature of this interaction in GCs that go on to activate immune cells. However, much can be learned by examining the binding energy of soluble forms of membrane-associated proteins to better understand the rates of these interactions. Therefore, I used a soluble form of ICOS (hICOS.Fc) and both a soluble and cell-associated form of ICOSL (sICOSL and hICOSL) to understand the kinetics of this interaction.

I first examined the soluble purified proteins using SPR in order to determine how the on and off rates contribute to the overall binding energy. To avoid inactivation of hICOS.Fc via direct immobilization on the SPR surface, hICOS.Fc surface was prepared by capture onto antihuman IgG (Figure 5A). The sICOSL binding curves shown in black (Figure 5B) show an initial rapid association, illustrated by a steep rise in binding at all concentrations, followed by a slower association phase rise over the remainder of the injection time. Samples at the highest concentrations were at or close to equilibrium near the end of the 120 s injection time. At the end of the injection, samples showed apparent 2-phase dissociation: an initial rapid decline, followed by a more gradual phase. Most samples did not return to baseline over the 360 s dissociation period.

This was unexpected because the shape of the binding curves did not match the shape expected of a 1:1 binding interaction. In addition, the fit to the data (shown in red) did not fit well to this model (Figure 5B). In fitting the data, I focused on the initial rapid dissociation phase, as the latter slow dissociation

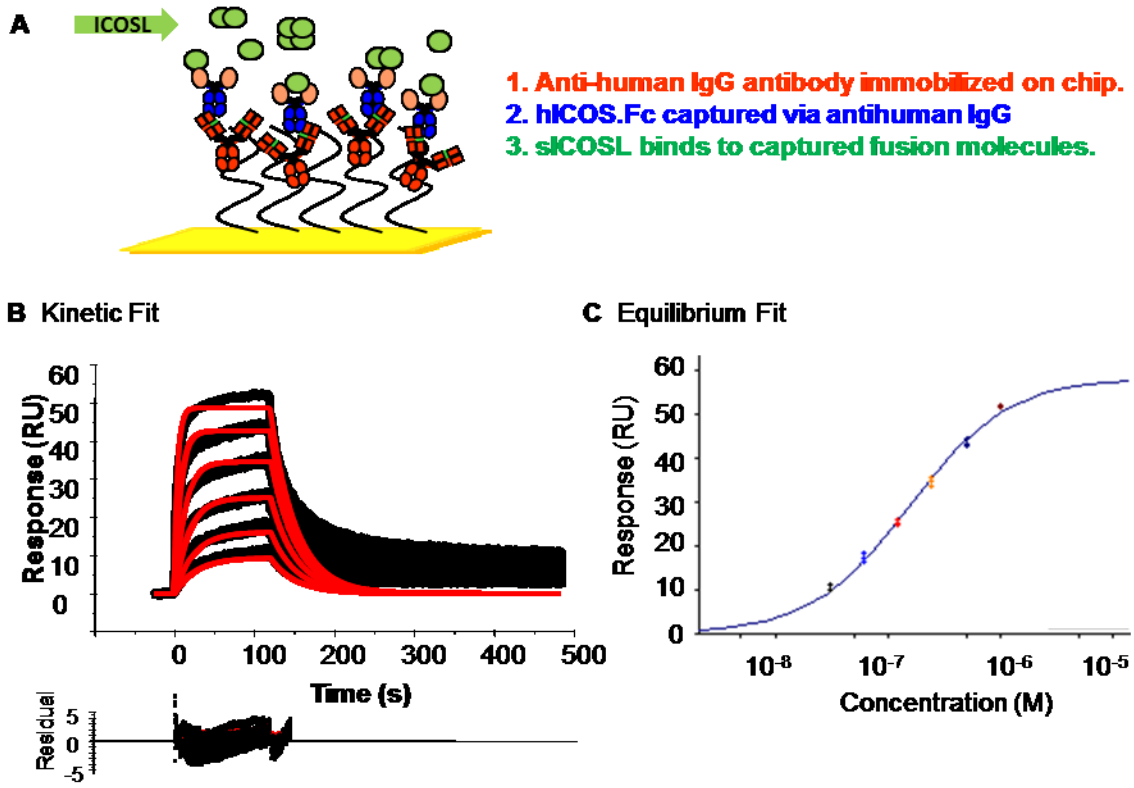

Figure 5. SPR Binding Experiments for hICOSL: hICOS.Fc Interaction. **A**. Preparation of the SPR surface to measure binding interaction. **B**. sICOSL was injected over captured hICOS.Fc at 1,000, 500, 250, 125, 62.5 and 31.25 nM. Data shown are 3 replicates with binding data in black and 1:1 fit in red. Residual plot shows distance between the fit data and raw data for a given time point for a given binding curve. **C**. Equilibrium K_D fit using 4 parameter logistical nonlinear regression model using binding data taken just before the end of the injection.

phase may be at least partially explained by an artifact of the surface-based measurement, which is rebinding of dissociated sICOSL molecules to other hICOS.Fc molecules on the surface. Mean values from intra-experimental triplicates acquired over three different binding surfaces (+/- the standard deviation) are 1.9 ($\pm$ 0.3) x 10^5 $M^{-1}s^{-1}$ for the k_a (on-rate), 3.0 ($\pm$ 0.1) x 10^{-2} s^{-1} for the k_d (off-rate), and 160 ($\pm$ 20) nM for the K_D (affinity). The average normalized

Pearson's chi-squared (χ^2/R_{max}) value, a measure of goodness of fit, from 3 independent surfaces was 5.3%. Additionally, the equilibrium K_D was calculated, and is approximately 170 ($\pm$30) nM (Figure 5C). As the kinetic fit does not truly reflect the raw data, the kinetic binding constants should not be considered as truly representative of this interaction. The poorness of fit of the overall binding curve to a 1:1 interaction indicates that this binding system may not be measuring a true binding affinity for a 1:1 interaction, and that a more complex interaction might be occurring between these two molecules. Further investigation of the oligomerization state of sICOSL is warranted based on this data to determine if the molecule used in this experiment is monomeric.

Protein Characterization

The poorness of fit to a 1:1 binding molecule was unexpected as sICOSL was expected to be monomeric and the SPR experiment was designed using low surface densities and with the bivalent hICOS.Fc on the surface in order to minimize rebinding effects. There are several potential reasons that could explain this. One plausible explanation is that one or both of the species involved in the interaction may not be a monomer. As the form of ICOS used in these experiments contains two extracellular binding domains of the ICOS molecule fused to an Fc domain, and as the SPR experiment was designed to measure a 1:1 interaction by capturing hICOS.Fc on the surface and using

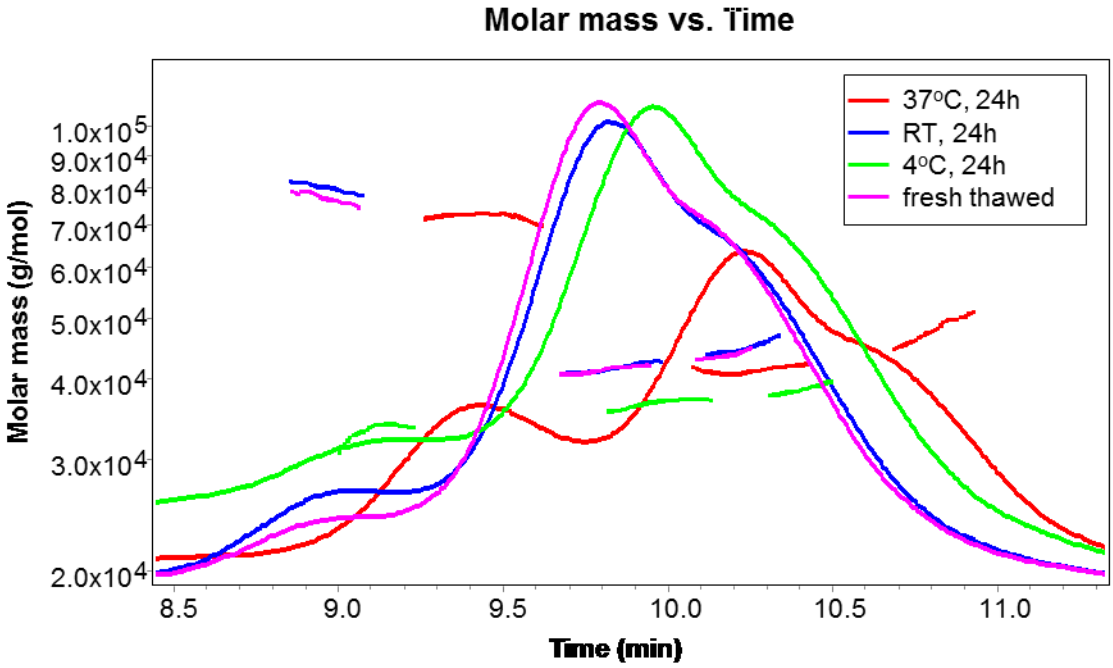

Figure 6. SEC-MALS characterization of sICOSL.

sICOSL in solution, the sICOSL protein should be further characterized to determine if it is a monomer.

Therefore, the purified recombinant sICOSL protein used for subsequent binding experiments was first characterized for the presence of dimeric *vs*. monomeric protein forms by SEC-MALS. Results from these experiments revealed three different peaks that corresponded to molecular weights of approximately 70 kDa, 40 kDa, and 45 kDa (Figure 6). Initial characterization following purification revealed a non-reduced molecular weight by SDS-PAGE of 40-66 kDa, likely reflecting glycosylation as the theoretical molecular weight of the protein is 25.4 kDa. Therefore, the 40 and 45 kDa peaks observed by SEC- MALS are

Table 1. SEC-MALS characterization of sICOSL

	Peak 1		Peak 2		Peak 3	
	MW (kDa)	**% mass**	**MW (kDa)**	**% mass**	**MW (kDa)**	**% mass**
0 hr	77	6.3%	41	53.8%	48	39.9%
4 C 24 hr	50	12.0%	39	49.0%	42	39.0%
RT 24 hr	78	9.2%	41	50.5%	44	40.3%
37 C 24 hr	71	28.3%	41	43.0%	47	28.7%

consistent with monomer forms that have slightly different glycosylation, whereas the 70 kDa peak is consistent with the size of a dimeric form. The percent mass recovery for the apparent dimeric 70 kDa peak varied from 6% in the freshly thawed sample to up to 28% in a sample that was incubated at 37^{o}C for 24 hours. The sample that most closely matches the conditions used in subsequent experiments of this study was incubated at room temperature for 24 hours. This showed 9% apparent 70 kDa dimeric species (Table 1).

These results may partially explain the poorness of fit to the 1:1 model from the SPR experiments. It appears that sICOSL has a propensity to form non-covalent dimers. This is consistent with evidence that ICOSL dimerizes on cell membranes (Chattopadhyay *et al*., 2006). ICOS is also known to form

homodimers on the membranes of T cells (Hutloff *et al*., 1999). Therefore, it is possible that the 1:1 binding affinity is not the most physiologically relevant binding parameter for this interaction, and that an avidity measurement in solution or on cells may be a better indicator of the biological interaction between these two molecules.

Measurement ICOS: ICOSL Binding Avidity

As the SPR binding data did not fit a typical 1:1 binding interaction, a second orthogonal technique was used to measure the K_D for the interaction between sICOSL and hICOS.Fc. Characterization of sICOSL revealed that the protein has a propensity to form dimers in solution over time, although the sICOSL protein alone is still predominantly monomeric. It is possible that when sICOSL is incubated with hICOS.Fc that this may increase the likelihood of dimer formation of sICOSL. A SEC-MALS experiment was performed to try to determine the stoichiometries of binding between these two proteins (data not shown), but there were too many overlapping peaks and results were difficult to decipher. The binding interaction between two dimers typically results in a higher functional affinity than the intrinsic affinity of two monomers as the dissociation of one domain does not necessarily coincide with the dissociation of the corresponding dimeric domain, resulting in an increased functional affinity, or avidity (Male *et al*. 2013: 57-58). If neither the recombinant nor the physiological forms of ICOS and ICOSL exist as monomers, then a measurement of the

Table 2. KinExA Signal Test Results. Results are from a single experiment run in duplicate. Signal is mean +/- the standard deviation. Net signal is signal for hICOS.Fc minus signal for blank.

	Signal	**Net Signal**
Azlactone		
Blank	0.0445 (± 0.009)	
100 pM hICOS.Fc	0.20 (± 0.01)	**0.16**
Sepharose		
Blank	0.129 (± 0.001)	
100 pM hICOS.Fc	0.313 (± 0.006)	**0.184**
PMMA		
Blank	0.0133 (± 0.0002)	
100 pM hICOS.Fc	0.124 (± 0.004)	**0.111**

binding avidity is more relevant than the binding affinity, and the avidity will likely be more potent than the 1:1 binding affinity.

KinExA, short for kinetic exclusion assay, is a complementary technique to SPR that can be used to measure binding interactions between two unlabeled soluble binding partners or between a soluble protein and a cell-surface protein. The first set of experiments was designed to determine which bead set gave the highest fluorescent signal when coated with sICOSL. Of the three bead sets that were tested, the sepharose beads gave the highest net signal when a solution of 100 pM hICOS.Fc was injected (*vs*. background binding) (Table 2). Further optimization of hICOSL coating concentration onto the beads and the volume of ICOS.Fc injected was performed in order to obtain a net signal within the linear detection range of 0.5 to 1.5 V (data not shown). Beads were coated with a

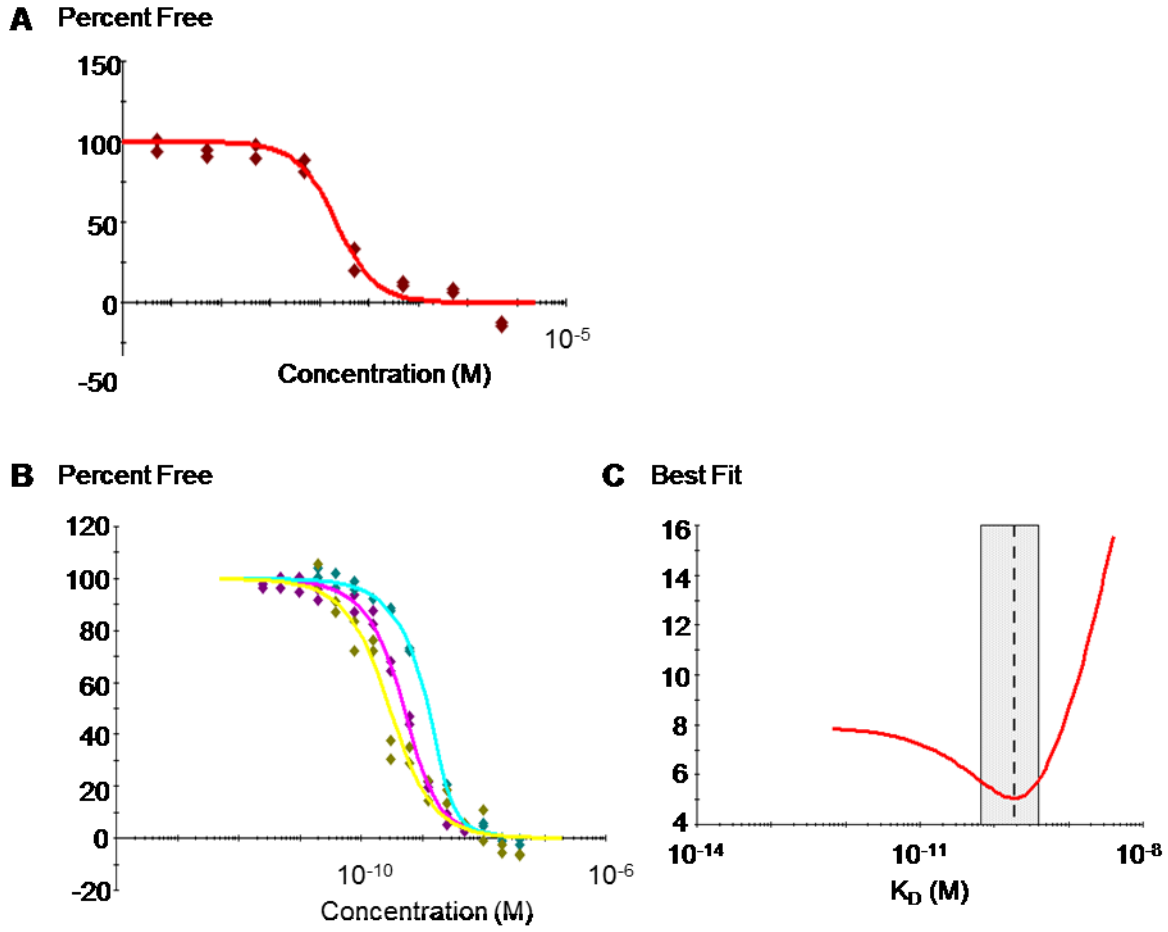

Figure 7. sICOSL binding to hICOS.Fc by KinExA. **A** Initial titration experiment over broad concentration range to estimate K_D for interaction and range of ligand concentrations required for K_D determination. **B** Combined analysis of 3 independent experiments at 50, 150, and 500 pM hICOS.Fc respectively, and with sICOSL titrated 2-fold from 40 nM to 2.44 pM. **C** K_D and 95% CI from combined analysis of 3 experiments.

higher concentration of hICOSL (50 μg/mL) for all experiments that were performed for measurement of K_D.

hICOS.Fc was prepared at a 150 pM and hICOSL was titrated 10-fold from 500 nM to 50 fM, as described in Methods. Equilibrated samples were run

in the KinExA system as described and detected via a Dylight649-conjugated antihuman secondary antibody (Jackson Immunoresearch). Concentration *vs*. fluorescence values were plotted and the K_D was estimated to be 183 pM with a 95% confidence interval (CI) of 660 fM to 443 pM (Figure 7A).

Based on the initial K_D estimate, subsequent experiments were performed to more precisely determine the K_D for the sICOSL: hICOS.Fc interaction. sICOSL was titrated using 2-fold dilutions over a narrower concentration range focused around the estimated K_D. Concentrations of hICOS.Fc were kept constant at either 50, 150, or 500 pM in three independent experiments. In order to obtain an accurate K_D measurement using KinExA, it is critical that the receptor concentration is close to or below the K_D value. When multiple curves are run at different receptor concentrations for the same interaction, curves may be analyzed together in order to obtain a more accurate determination of the K_D. Concentration *vs*. fluorescence plots were generated for each independent experiment, as in Figure 7A. Data from all three experiments was combined in order to obtain a more accurate determination of the K_D for the binding system (Figure 7B). The K_D from this combined analysis is 190 pM with a 95% CI from 65 to 394 pM (Figure 7C).

As ICOSL is expressed on the cell surface of APCs, KinExA was also used to measure the binding interaction between hICOS.Fc and hICOSL expressed on CHO DR2 cells. Cells were titrated from 1.217×10^7 cells/mL 2-fold down to 5 cells/mL, as described in Methods, at 100 pM or 2 nM hICOS.Fc.

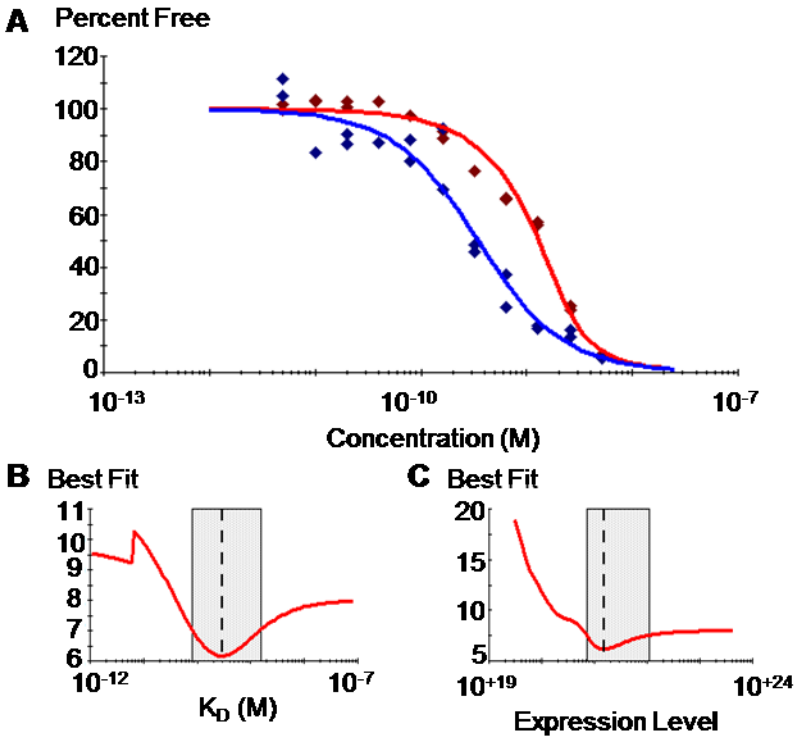

Figure 8. Affinity Determination on hICOSL expressing CHO DR2 cells. **A** Combined analysis of two curves prepared at the same time from the same batch of cells using two different concentrations of hICOS.Fc. **B** K_D and 95% CI from whole cell analysis. **C** Expression level from whole cell analysis.

To determine the K_D of binding for hICOSL to hICOS.Fc, concentration *vs*. fluorescence curves were fit individually and then plotted together using the whole cell analysis to determine the expression level of hICOSL on the CHO DR2 cells and the K_D (Figure 8A). The K_D from this analysis is 296 pM with a 95% CI from 81 pM to 2 nM (Figure 8B). The expression level is 2×10^{21} molecules hICOSL/cell with a 95% CI from 7×10^{20} to 1×10^{21} molecules/cell (Figure 8C). No binding was observed to the negative control CHO DR2 parental cell line that does not express hICOSL, as expected (data not shown).

The confidence intervals for the cell-based binding data are higher than ideal. The primary source of variability in this data is likely due to the behavior of the cells during the overnight incubation with hICOS.Fc that is required in order for the binding system to reach equilibrium. Visualization of cell viability using Trypan blue following the overnight incubation of cells with hICOS.Fc reveals that there is some cell death that occurs during the overnight incubation of hICOSL-expressing CHO cells with hICOS.Fc. However, the fact that the K_D is so similar to the solution-based K_D lends confidence to this data.

DISCUSSION

The ICOS: ICOSL interaction is implicated in SLE pathogenesis; yet there are several aspects of the biology of this interaction that are poorly understood. Among these are the overall potency of the binding interaction of both the shed and transmembrane forms of ICOSL with ICOS on T cells, the function of shed ICOSL, and the biological effects of reverse signaling in humans. Developing an improved understanding of the biology of this interaction is useful in order to determine whether targeting this interaction may be a viable therapeutic approach for the treatment of SLE. The hypothesis evaluated in this study was that the ICOS: ICOSL interaction is a potent and critical mediator of proinflammatory signaling and immune activation that functions both via activated T cell-mediated forward signaling and APC-mediated reverse signaling mechanisms and that ectodomain shedding of ICOSL is a protective mechanism that leads to down-regulation of the proinflammatory signaling cascade initiated by this interaction.

The binding interaction between recombinant soluble human ICOSL and recombinant hICOS.Fc was interrogated using two complimentary technology platforms, a surface based biosensor (Biacore) and a solution-based biosensor (KinExA). Both platforms measure binding rates without the need for labeling the proteins. SPR detection is based on the addition of mass to the sensor chip surface due to binding. Binding of sICOSL to hICOS.Fc was detected as response in real time, allowing for direct measurement of binding rates (k_a, k_d)

and calculation of the binding affinity (K_D). Based on the experimental design (Figure 5A), where bivalent hICOS.Fc was captured on the sensor chip surface at relatively low immobilization densities and based on the assumption that the expressed recombinant sICOSL that was injected over the surface was homogenous and monomeric, one would have expected that the kinetics of this interaction would have fit well to a 1:1 binding model. The association and dissociation rates fit poorly to this model, however. Therefore the affinity of this interaction could not be accurately determined.

There are several possibilities that could explain the poor fit of the data to the expected binding model. Protein characterization using SEC-MALS revealed that the sICOSL was not solely monomeric, and that the protein had a tendency to dimerize in solution over time and with increasing temperatures. Given the propensity of the molecule to dimerize in solution, it is possible if not likely that when two sICOSL molecules are brought into close proximity with one another by binding to separate arms of the bivalent hICOS.Fc molecule that increased dimerization may have occurred. If this is the case then the rate of dissociation would no longer be driven by a single sICOSL molecule binding with a single binding site on hICOS.Fc. It would instead be complicated by the strength of multiple binding interactions. Since neither sICOSL nor hICOS.Fc is a true monomer, it was impossible to measure the intrinsic binding affinity of a 1:1 interaction.

An advantage of the KinExA platform in comparison to SPR is that both molecules being studied can interact freely in solution. KinExA was used to measure the K_D of the hICOSL: hICOS.Fc interaction when both molecules were in solution, or when hICOSL was expressed on the surface of CHO DR2 cells. The two different KinExA systems that were run showed similar K_D values of approximately 190 pM when both molecules were in solution and approximately 300 pM when hICOSL was on the surface of CHO DR2 cells. For reasons described above, these K_Ds probably do not reflect a true 1:1 affinity value, but likely reflect the effect of avidity due to multiple binding partners interacting with different parts of the larger overall molecules to create a tighter overall interaction.

Based on the fact that ICOS is known to exist on T cells as a disulfide-linked dimer and that ICOSL has been shown to dimerize on the surface of APCs, the avidity that is measured by KinExA, may approximate a relevant functional affinity for this interaction *in vivo*. It would be interesting to test this interaction on more biologically relevant cell systems. Unfortunately due to the sensitivity limits of the KinExA instrument, it is not possible to measure the interaction with ICOS expressed on T cells or with ICOSL on APCs such as B cells or dendritic cells, due to the relatively low expression of ICOSL on the surface of these cells. High-expressing cells at high concentrations, in large quantities, and often at high injection volumes are requirements for successfully measuring such an interaction using the KinExA platform.

The K_D that was determined using KinExA was almost 1,000-fold tighter that the K_D that was determined using SPR. Similar discrepancies between the binding affinity measured using SPR and the avidity measured using KinExA were observed in a study that looked at binding of various anti-TNF molecules to soluble TNF (sTNF), which is a costimulatory molecule that is found in solution as a trimer. In this case, avidity measurements by KinExA are 10-20 fold stronger than affinity measurements by SPR (Kaymakcalan *et al*., 2009). In both the case of sTNF and sICOSL, what may be happening is that as these costimulatory ligands bind to their receptors, the oligomerization states of the molecules allow for formation of multivalent immune complexes on the KinExA platform due to the freely interacting molecules in solution that are unable to form when a single molecule is captured at a low density on the SPR surface. In Biacore experiments the maximum avidity effect that could be measured would most likely be due only to the interaction between two dimers, whereas on KinExA, the avidity effect could be due to the interaction with multivalent complexes of these molecules. The dissociation of these larger complexes would be slower, due to multiple binding interactions that keep the overall complex associated, leading to a higher avidity.

Thus, the binding affinity of monomeric ICOSL may not be the most relevant indicator of the true *in vivo* binding interaction between ICOS and ICOSL either in its shed form or on APCs. All of this data suggests that the functional binding affinity for the ICOS: ICOSL interaction may be the accumulated strength

of multiple non-covalent binding interactions. Results indicate that the functional binding affinity is significantly higher than the intrinsic affinity previously measured. In lupus patients with higher levels of sICOSL in plasma signaling through ICOS: ICOSL is likely intensified due to the improper classification of self-antigens as foreign. In this case, it may be important to inhibit this interaction in order to reduce the inflammatory cascade initiated through this interaction that leads to the production of destructive autoantibodies.

Future Directions

As previously described, there is genetic, cellular, and proteomic evidence for the role of ICOS and ICOSL in SLE. Developing a better understanding of the role of reverse signaling caused by ICOS on T cells binding to ICOSL on APCs could lead to an improved understanding of the ideal approach for targeting this interaction therapeutically. While some data suggests that reverse signaling occurs in mouse DCs via ICOS.Ig stimulation of ICOSL (Tang *et al*., 2009) there is not sufficient evidence that reverse signaling occurs via this interaction in humans. Thus, additional research could extend the experiments performed in mouse DCs to human APCs, such as DCs or B cells, to confirm whether ICOS.Ig stimulation up- or down-regulates cytokine production in APCs. Recombinant forms of ICOSL could be expressed on an APC cell line of the two different ICOSL splice variants (GL50 and B7-H2) to determine whether the 10 additional amino acids found in the more selectively expressed GL50 variant (found in

leukocytes, spleen, and lymph node tissue) are required in order to initiate this reverse signaling cascade *vs*. the ubiquitously expressed B7-H2 variant.

The homologous molecule CTLA-4 has been shown to be effective therapeutically via its effects on both classical and reverse signaling pathways. As previously mentioned, CTLA-4 performs an inhibitory function on T cells by binding the CD28 ligands B7-1 and B7-2 with a higher affinity than CD28 (van der Merwe *et al*., 1997) thus inhibiting classical signaling through CD28 and activation of naïve T cells. Abatacept, or CTLA-4.Ig, is effective due to its inhibition of signaling through CD28. A secondary effect was also discovered whereby abatacept initiates reverse signaling in APCs, inducing the transcription of IFN-γ, which activates IDO and thereby increases Trp catabolism, leading to decreased T cell proliferation (Grohmann *et al*., 2002). This unintended secondary effect of abatacept fortunately also serves an immunosuppressive function.

If inflammatory signaling is observed in APCs due to ICOS.Ig stimulation, then a preferred therapeutic approach may be the development of an antibody targeting either ICOS or ICOSL, which would not have the secondary effect of reverse signaling. However, if the reverse signaling effect via ICOSL is found to be beneficial, one could envision an approach similar the CTLA-4.Ig therapeutic whereby ICOS.Ig is administered in order to initiate the reverse signaling cascade while simultaneously inhibiting the pro-inflammatory classical signaling cascade through ICOS on T cells. The safety of such a molecule would need to

be thoroughly evaluated prior to administering this treatment in humans, however, as this would likely exacerbate inflammatory effects due to forward signaling mechanisms through ICOS on T cells.

ICOSL is the only B7 family member that is known to be shed and the protease responsible for the induction of shedding is unknown. Logue *et al*. (2006) revealed that ICOSL is rapidly shed following ICOS binding and B cell receptor (BCR) engagement. Using molecular biology techniques, the authors swapped out various domains of ICOSL with domains of the unsheddable costimulatory ligand B7-2. They determined that shedding can be induced by phorbol-12-myristate-13-acetate (PMA) and by ICOS. Treatment with the hydroxamate inhibitor, GM6001, a pan-metalloproteinase binder, completely inhibited shedding induced by PMA, but not shedding induced by ICOS. The stalk region of ICOSL that connects the IgC domain to the transmembrane region was determined to be necessary for ectodomain shedding following PMA treatment. In contrast, ICOS-induced shedding appears to involve the stalk and IgC domains of ICOSL. The proteases responsible for both shedding mechanisms remain to be identified.

It is unclear whether shed ICOSL exacerbates the autoimmune disease phenotype or serves a protective role. Her *et al*.(2009) have shown that increased levels of soluble ICOSL are observed in human patients with active SLE compared to patients with inactive SLE, RA patients, and healthy controls.

This increase in shed ICOSL corresponds to a decrease in membrane-bound ICOSL on APCs, and no change in mRNA levels of ICOSL.

Future experiments could be designed to specifically interrogate whether the shedding of ICOSL is a protective mechanism or a disease-exacerbating mechanism in SLE patients. Existing evidence indicates that it may play a protective role by decreasing costimulatory signaling through ICOS and thus the production of downstream inflammatory cytokines; however that remains to be proven. Based on evidence implicating both ICOS and ICOSL in SLE pathogenesis, both molecules may be interesting therapeutic targets for SLE treatment. Acquiring a better understanding of whether shed ICOSL is protective or pathogenic could lead to a preferential targeting of one form of the protein. Work could also be performed to better understand the protease(s) responsible for the shedding of ICOSL. Depending on the specificity of a given protease for ICOSL cleavage *vs*. other membrane proteins, design of an agonist or antagonist of that protease could also be considered as a therapeutic approach.

Answering these fundamental biological questions could help to address the question of whether an inhibitor to ICOS or ICOSL could be a viable therapeutic for the treatment of SLE. However, *in vitro* experiments and mouse models of SLE are inherently limited in their ability to model a very complex and heterogeneous human disease. Thus, effectiveness in any preclinical system may help us to understand some of the nuances of the biology of this interaction, but are unlikely to lead to a true and complete understanding of the human

disease and aspects thereof. Ultimately, the human experiment will need to be performed in order to truly answer this question. However, understanding efficacy in SLE is not trivial. Clinical trials must be carefully designed to account for the vast heterogeneity of the disease and to protect patients from its devastating effects, including organ damage. This often involves enrolling patients who are already taking concomitant therapies and either tapering these therapies or establishing an effect of the experimental drug that is in addition to the background therapeutics of patients. Treatment periods must typically be at least 6 months in order to observe symptomatic changes.

A number of small and large molecules are currently being evaluated for the treatment of SLE. B-cell-directed therapies target CD19, CD20, CD22, CD40 and FcγRIIB. These approaches generally attempt to deplete B cells or to inhibit their function. T-cell-directed therapies do not aim for T cell depletion, but to promote T cell tolerance, block T cell activation and differentiation, and inhibit T cell trafficking. Targets for T-cell inhibition include CTLA-4, CD40L, and ICOSL. Cytokines are relevant in SLE due to their role in the generation and maintenance of inflammation. Cytokine-directed therapies including agents targeting B cell activating factor (BAFF), type I interferons, IL-6 or TNF are also being evaluated (Stohl, 2013).

Monoclonal antibodies (mAbs) are being developed against ICOSL to inhibit the ICOS: ICOSL interaction. The goal here is to inhibit the differentiation of activated T cells into differentiated T_{FH} cells, which are important in the

maturation of B cells into antibody-producing cells in germinal centers. Two Phase 1 clinical studies have been initiated using anti-ICOSL mAbs. It will likely be several years before we learn whether these molecules are effective in the treatment of SLE (Stohl, 2013).

Choosing the right groups of SLE patients may also be critical to running a successful clinical study. For example, it would be difficult to remove background medications from patients with the most severe forms of SLE due to safety risks. However, it may be difficult to observe a measurable effect in those patients with the mildest form of the disease. Therefore, patients who have moderate SLE may be good candidates for a clinical trial that attempts to taper and/or remove background medications in order to most clearly observe the effect of the study drug.

It will also be important to evaluate a number of systemic biomarkers in addition to the clinical endpoints such as SLEDAI, BILAG, or SRI. Meaningful biomarkers for a therapy targeting ICOSL would likely be T cells and B cells, which can be measured by flow cytometry. Safety biomarkers such as neutrophil levels and viral load levels should also be evaluated in order to determine safety risks prior to occurrence of adverse safety-related events due to too much immune suppression. It would be useful to attempt to stratify subgroups of patients within a clinical study by measuring biomarkers such as autoantibody reactivities and levels prior to enrollment and at several time points during the course of treatment in order to determine if further stratification is needed.

Finally it would be useful to measure genes and proteins that are indicative of the overall level of inflammation such as interferon-modulated genes and proteins and measurable pro- and anti-inflammatory cytokines and chemokines. In particular, levels of soluble ICOSL in patients' serum could be measured at baseline as a potential patient stratification marker to determine whether patients with higher levels of sICOSL respond more or less favorably to therapy. sICOSL could also be measured longitudinally to determine whether levels increased or decreased due to treatment and/or a reduction in SLE disease activity.

Due to the heterogeneity of SLE, it is unlikely that any one therapeutic approach that is pursued will provide an optimal and effective treatment for all SLE patients. It is more likely that subsets of patients with common molecular and clinical phenotypes will benefit from different subsets and/or combinations of these therapies. Among the major challenges that remain will be to properly design ongoing and future clinical studies in order to target the subsets of patients that will most benefit from a given therapy and choosing meaningful and attainable trial endpoints in order to differentiate therapies with the potential to ameliorate this devastating disease from those that are ineffective.

APPENDIX

Amino Acid Symbols

Full Name	3-Letter Symbol	1-Letter Symbol
Alanine	Ala	A
Arginine	Arg	R
Asparagine	Asn	N
Aspartic Acid	Asp	D
Cysteine	Cys	C
Glutamic Acid	Glu	E
Glutamine	Gln	Q
Glycine	Gly	G
Histidine	His	H
Isoleucine	Ile	I
Leucine	Leu	L
Lysine	Lys	K
Methionine	Met	M
Phenylalanine	Phe	F
Proline	Pro	P
Serine	Ser	S
Threonine	Thr	T
Tryptophan	Trp	W
Tyrosine	Tyr	Y
Valine	Val	V

REFERENCES

Aicher A, Hayden-Ledbetter M, Brady WA, Pezzutto A, Richter G, Magaletti D, Buckwalter S, Ledbetter JA, Clark EA. Characterization of Human Inducible Costimulator Ligand Expression and Function. *The Journal of Immunology*. 2000; 164: 4689-4696.

Amour A, Slocombe PM, Webster A, Butler M, Knight CG, Smith BJ, Stephens PE, Shelley C, Hutton M, Knauper V, Docherty AJP, Murphy G. TNF-α converting enzyme (TACE) is inhibited by TIMP-3. *FEBS Letters*. 1998; 435(1): 39-44.

Arribas J, Borroto A. Protein Ectodomain Shedding. *Chemical Reviews*. 2002; 102(12): 4627-4638.

Assessing the Cost of Lupus. [Internet]. [cited 2014 March 26]. Available from http://www.lupusresearch.org/research/lru/assessing_cost.html

B6.129P2-*Icosl*$^{tm1Mak/J}$. [Internet]. [cited 2014 March 21]. Available from http://jaxmice.jax.org/strain/004657.html

Brodie D, Collins AV, Iaboni A, Fennelly JA, Sparks LM, Xu X-N, van der Merwe PA, David PA. LICOS, a primordial costimulatory ligand? *Current Biology*. 2000; 10: 333-336.

Chambers C. The expanding world of co-stimulation: the two-signal model revisited. *TRENDS in Immunology*. 2001; 122(4): 217-223.

Chattopadhyay K, Bhatia S, Fiser A, Almo SC, Nathenson SG. Structural Basis of Inducible Costimulator Ligand Costimulatory Function: Determination of the Cell Surface Oligomeric State and Functional Mapping of the Receptor Binding Site of the Protein. *The Journal of Immunology*. 2006; 177: 3920-3929.

Collins AV, Brodie DW, Gilbert RJC, Iaboni A, Manso-Sancho R, Walse B, Stuart DI, van der Merwe PA, Davis SJ. The Interaction Properties of Costimulatory Molecules Revisited. *Immunity*. 2002; 17: 201-210.

Coyle AJ, Lehar S, Lloyd C, Tian J, Delaney T, Manning S, Nguyen T, Burwell T, Schneider H, Gonzalo JA, Gosselin M, Owen LR, Rudd CE, Gutierrez-Ramos JC. The CD28-Related Molecule ICOS is Required for Effective T Cell-Dependent Immune Response. *Immunity*. 2000; 13(1): 95-105.

Cunninghame Graham DS, Wong AK, McHugh NJ, Whittaker JC, Vyse TJ. Evidence for unique association signals in SLE at the *CD28-CTLA4-ICOS* locus in a family-based study. *Human Molecular Genetics*. 2006; 15(21): 3195-3205.

Elmore S. Apoptosis: A Review of Programmed Cell Death. *Toxicologic Pathology*. 2007; 35: 495-516.

Gizinski AM, Fox DA, Sarkar S. Co-stimulation and T cells as therapeutic targets. *Best Practice & Research Clinical Rheumatology*. 2010; 24: 463-477.

Greenwald RJ, Freeman GJ, Sharpe AH. The B7 Family Revisited. *Annual Review of Immunology*. 2005; 23: 5115-548.

Grohmann U, Orabona C, Fallarino F, Vacca C, Calcinaron F, Falorni A, Candeloro P, Belladonna ML, Bianchi R, Fioretti MC, Puccetti P. CTLA-4-Ig regulates tryptophan catabolism *in vivo*. *Nature Immunology*. 2002; 3(11): 1097-1101.

Hahn B. Targeted therapies in systemic lupus erythematosus: successes, failures and future. *Annals of the Rheumatic Diseases*. 2011; 70(Supplement 1): i64-66.

Heissmeyer V, Ansel KM, Rao A. A plague of autoantibodies. *Nature Immunology*. 2005; 6(7): 642-644.

Her M, Kim D, Oh M, Jeong H, Choi I. Increased expression of soluble inducible costimulator ligand (ICOSL) in patients with systemic lupus erythematosus. *Lupus*. 2009; 18: 501-507.

Hutloff A, Buchner K, Reiter K, Baelde HJ, Odendahl M, Jacobi A, Dorner T, Kroczek RA. Involvement of Inducible Costimulator in the Exaggerated Memory B Cell and Plasma Cell Generation in Systemic Lupus Erythematosus. *Arthritis & Rheumatism*. 2004; 50(10): 3211-3220.

Hutloff A, Dittrich AM, Beier KC, Eljaschewitsch B, Kraft R, Anagnostopoulos I, Kroczek RA. ICOS is an inducible T-cell co-stimulator structurally and functionally related to CD28. *Nature*. 1999; 397: 263-266.

Kaymakcalan Z, Sakorafas P, Bose S, Scesney S, Xiong L, Hanzatian DK, Salfeld J, Sasso EH. Comparisons of affinities, avidities, and complement activation of adalimumab, infliximab, and etanercept in binding to soluble and membrane tumor necrosis factor. *Clinical Immunology*. 2009; 131: 308-316.

Kremer JM, Genant HK, Moreland LW, Russell AS, Emery P, Abud-Mendoza C, Szechinski J, Li T, Ge Z, Becker J-C, Westhovens R. Effects of Abatacept in Patients with Methotrexate-Resistant Active Rheumatoid Arthritis. *Annals of Internal Medicine*. 2006; 144: 865-876.

Ling V, Wu PW, Finnerty HF, Bean KM, Spaulding V, Fouser LA, Leonard JP, Hunter SE, Zollner R, Thomas JL, Miyashiro JS, Jacobs KA, Collins M. Cutting Edge: Identification of GL50, a Novel B7-Like Protein That Functionally Binds to ICOS Receptor. *The Journal of Immunology*. 2000; 164: 1653-1657.

Ling V, Wu PWW, Miyashiro JS, Marusic S, Finnerty HF, Collins M. Differential Expression of Inducible Costimulator-Ligand Splice Variants: Lymphoid Regulation of Mouse GL50-B and Human GL50 Molecules. *The Journal of Immunology*. 2001; 166: 7300-7308.

Logue EC, Bakkour S, Murphy MM, Nolla H, Sha WC. ICOS-Induced B7h Shedding on B Cells in Inhibited by TLR7/8 and TLR9. *The Journal of Immunology*. 2006; 177: 2356-2364.

Liu Y, Zhu T, Cai G, Qin Y, Wang W, Tang G, Zhao D, Shen Q. Elevated circulating $CD4^{+}ICOS^{+}Foxp3^{+}$ T cells contribute to overproduction of IL-10 and are correlated with disease severity in patients with systemic lupus erythematosus. *Lupus*. 2011; 20: 620-627.

Luijten KMAC, Tekstra J, Bijlsma JWJ, Bijl M. The Systemic Lupus Erythematosus Responder Index (SRI); A new SLE disease activity assessment. *Autoimmunity Reviews*. 2012; 11: 326-239.

Male D, Brostoff J, Roth DB, Roitt IM. Immunology. 8th edition. 2013. Elsevier. 57-58 p.

McAdam AJ, Greenwald RJ, Levin MA, Chernova T, Malenkovich N, Ling V, Freeman GJ, Sharpe AH. ICOS is critical for CD40-mediated antibody class switching. *Nature*. 2001; 409: 102-105.

Mestas J, Hughes CCW. Of Mice and Not Men: Differences between Mouse and Human Immunology. *The Journal of Immunology*. 2004; 172(5): 2731-2738.

Motulsky HJ. GraphPad Prism Version 5.0 Regression Guide. 2007. GraphPad Software Inc., San Diego CA, www.graphpad.com

Murphy K, Travers P, Walport M. Janeway's Immunobiology. 7th edition. New York, NY. Garland Science, Taylor & Francis Group, LLC. 324-325, 345-347 p.

Myszka DG. Improving biosensor analysis. *Journal of Molecular Recognition.* 1999; 12: 279-284.

Önell A, Andersson K. Kinetic determinations of molecular interactions using Biacore - minimum data requirements for efficient experimental design. *Journal of Molecular Recognition.* 2005; 18: 307-317.

Orabona C, Grohmann U, Belladonna ML, Fallarino F, Vacca C, Bianchi R, Bozza S, Volpi C, Salomon BL, Fioretti MC, Romani L, Puccetti P. CD28 induces immunostimulatory signals in dendritic cells via CD80 and CD86. *Nature Immunology*. 2004; 5(11): 1134-1142.

Quintero OL, Amador-Patarroyo MJ, Montoya-Ortiz G, Rojas-Villaraga A, Anaya J-M. Autoimmune disease and gender: Plausible mechanisms for the female predominance of autoimmunity. *Journal of Autoimmunity*. 2012; 28: J109-J119.

Scholz C, Patton KT, Anderson DE, Freeman GJ, Hafler DA. Expansion of Autoreactive T Cells in Multiple Sclerosis Is Independent of Exogenous B7 Costimulation. *The Journal of Immunology*. 1998; 160: 1532-1538.

Schwartz RH. T cell anergy. *Annual Review of Immunology*. 2003; 21: 305-334.

Simpson TR, Quezada SA, Allison JP. Regulation of CD4 T cell activation and effector function by inducible costimulator (ICOS). *Current Opinion in Immunology*. 2010; 22: 1-7.

Stohl W. Future prospects in biologic therapy for systemic lupus erythematosus. *Nature Reviews Rheumatology*. Advance online publication 10 September 2013.

Systemic Lupus Erythematosus. [Internet]. [cited 2014 March 26]. Available from http://en.wikipedia.org/wiki/Lupus#Prognosis

Systemic Lupus Erythematosus (Lupus). [Internet]. [cited 2014 February 2]. Available from www.rheumatology.org/practice/clinical/patients/diseases_and_conditions_lupus.asp

Tang G, Qin Q, Zhang P, Wang G, Liu M, Ding Q, Qin Y, Shen Q. Reverse signaling using an inducible costimulator to enhance immunogenic function of dendritic cells. *Cell and Molecular Life Sciences*. 2009; 66: 3067-3080.

van der Merwe PA, Bodian DL, Daenke S, Linsley P, Davis SJ. CD80 (B7-1) Binds Both CD28 and CTLA-4 with a Low Affinity and Very Fast Kinetics. *The Journal of Experimental Medicine*. 1997; 185(3): 393-403.

Waterhouse P, Penninger JM, Timms E, Wakeham A, Shahinian A, Lee KP, Thompson CB, Griesser H, Mak TW. Lymphoproliferative Disorders with Early Lethality in Mice Deficient in *Ctla-4*. *Science*. 1995; 270(5238): 985-988.

What is lupus? [Internet]. [cited 2014 March 26]. Available from http://www.lupus.org/answers/entry/what-is-lupus

Yu D, Tan AH-M, Hu X, Athanasopoulos V, Simpson N, Silva DG, Hutloff A, Giles KM, Leedman PJ, Lam KP, Goodnow CC, Vinuesa CG. Roquin represses autoimmunity by limiting inducible T-cell co-stimulator messenger RNA. *Nature*. 2007; 450: 299-304.

Zhiping C, Zhenfu L, Zheng S, Liang Z. Expression of Inducible Co-stimulator in peripheral blood T lymphocytes in the patients with systemic lupus erythematosus. *Journal of Huazhong University of Science and Technology*. 2005; 25(3): 357-359.

CURRICULUM VITAE